Quaternary Science Reviews 27 (2008) 2076–2090

Contents lists available at ScienceDirect

Quaternary Science Reviews

journal homepage: www.elsevier.com/locate/quascirev

The development of blowouts and foredunes in the Ilha Comprida barrier (Southeastern Brazil): the influence of Late Holocene climate changes on coastal sedimentation

A.O. Sawakuchi [a,*], R. Kalchgruber [b,1], P.C.F. Giannini [a], D.R. Nascimento, Jr. [a], C.C.F. Guedes [a], N.K. Umisedo [c,2]

[a] Departamento de Geologia Sedimentar e Ambiental, Instituto de Geociências da Universidade de São Paulo, Rua do Lago, 562, São Paulo-SP 05508-080, Brazil
[b] Radiation Dosimetry Laboratory, Department of Physics, Oklahoma State University, 1110 South Innovation Way Drive, Stillwater, OK 74074, USA
[c] Laboratório de Dosimetria, Departamento de Física Nuclear, Instituto de Física da Universidade de São Paulo, Rua do Matão, 187, São Paulo-SP 05315-970, Brazil

ARTICLE INFO

Article history:
Received 28 February 2008
Received in revised form 20 August 2008
Accepted 29 August 2008

ABSTRACT

Middle to Late Holocene barriers are conspicuous landforms in southeastern and southern Brazilian regions. The barriers in the coastal zones of northern Santa Catarina, Paraná and São Paulo states (27°19′–24°00′S) are formed mainly by beach ridge alignments and many barriers present foredune and blowout alignments in their seaward portion. The development of these eolian landforms appears to record a regional shift in coastal dynamics and barrier building. In this context, the Ilha Comprida barrier stands out for its well-developed and well-preserved foredunes and blowouts. Based on the presence or not and type of eolian landforms, the Ilha Comprida barrier can be divided seaward into inner, middle and outer units. The inner unit is formed entirely by beach ridges. The middle unit comprises a narrow belt of blowouts (up to 15 m high) aligned alongshore. Blowout lobes pointing NNW are indicative of their generation by southern winds. The outer unit is represented by low ($\leq$1 m high) active or stabilized foredunes and a small transgressive dunefield ($\sim$1 km^2). Twenty-seven luminescence ages (SAR protocol) obtained for the beach ridges, foredunes, and blowouts of these three units allow definition of a precise chronology of these landforms and calculation of rates of coastal progradation. The inner unit presents ages greater than 1004 $\pm$ 88 years. The blowouts of the middle unit show ages from 575 $\pm$ 47 to 172 $\pm$ 18 years. The ages of the outer unit are less than 108 $\pm$ 10 years. Rates of coastal progradation for the inner and outer units are 0.71–0.82 m/year and 0.86–2.23 m/year, respectively. The main phase of blowout development correlates well with the Little Ice Age (LIA) climatic event. These results indicate that southern winds in subtropical Brazil became increasingly more intense and/or frequent during the LIA. These conditions persist to the present and are responsible for the development of the eolian landforms in the outer unit. Thus, barrier geomorphology can record global climatic events. The sensitivity of barrier systems in subtropical Brazil to Late Holocene climate changes was favored by the relative sea level stillstand during this time. Luminescence dating makes it possible to analyze barrier geomorphology during Late Holocene climate changes operating on timescales of a hundred to thousand years. These results improve our knowledge of barrier building and will help in the evaluation of the impact of future climate changes on coastal settings.

1. Introduction

Understanding coastal sedimentation during the Late Holocene on a centennial to millennial timescale, with reliable age information, is necessary to support prediction models about the impact of future climate and relative sea level changes on coastal settings. The dynamics of first-order coastal systems (systems operating on a 10^2 to 10^3 years sensu Cowell et al., 2003a) is of primary importance for coastal management because it controls systematic trends of coastline migration and morphology as well as the response of coastal zones to short-time events like storms (Cowell et al., 2003b).

* Corresponding author. Tel.: +55 11 3091 1989; fax: +55 11 3091 4207.
E-mail addresses: andreos@usp.br (A.O. Sawakuchi), regina.kalchgruber@okstate.edu (R. Kalchgruber), pcgianni@usp.br (P.C.F. Giannini), danieljr@usp.br (D.R. Nascimento Jr.), ccfguedes@yahoo.com.br (C.C.F. Guedes), numisedo@usp.br (N.K. Umisedo).
[1] Tel.: +1 405 744 1013; fax: +1 405 744 1112.
[2] Tel.: +55 11 3091 6975; fax: +55 11 3091 2742.

0277-3791/$ – see front matter © 2008 Elsevier Ltd. All rights reserved.
doi:10.1016/j.quascirev.2008.08.020

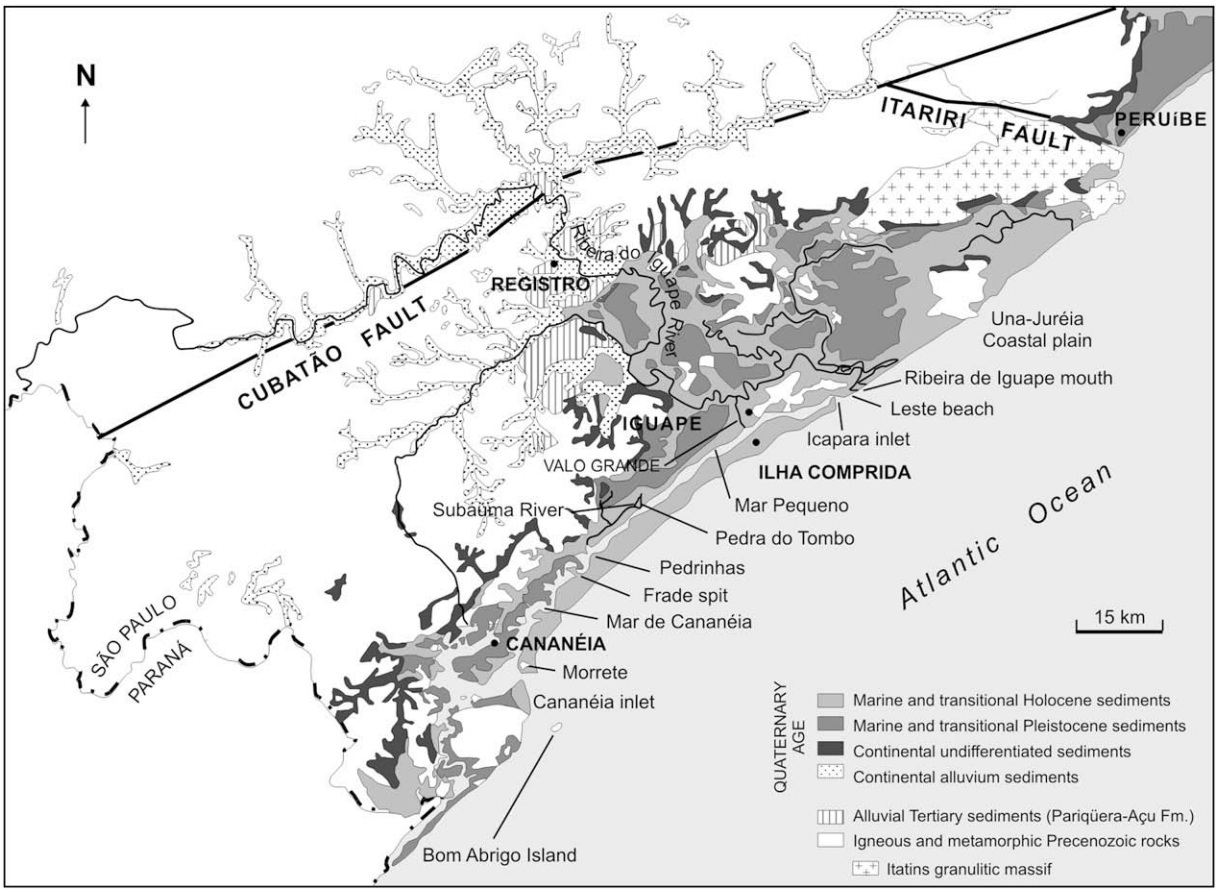

Fig. 1. Localization of the Ilha Comprida barrier. Adapted from Nascimento (2006) and Giannini et al. (2008).

Middle to Late Holocene barriers are frequent landforms along the most populated southeastern and southern Brazilian regions. The barriers in the coastal zones of northern Santa Catarina, Paraná and São Paulo states (27°19′–24°00′S) are formed mainly by beach ridge alignments and many barriers present foredune and blowout alignments in their seaward portion. The development of these eolian landforms appears to record a regional shift in coastal dynamics and barrier building. Dating studies dealing with the evolution of these Holocene Brazilian barriers on a timescale of few thousands to hundreds years are still scarce. Improved luminescence dating procedures (Duller, 1995; Murray and Wintle, 2000; Wintle and Murray, 2006) provide now a means to determine a more precise chronology of Quaternary depositional events, giving new insights into the dynamics of depositional systems. A suitable technique for dating of Holocene coastal depositional systems is optically stimulated luminescence (OSL) (Murray-Wallace et al., 2002; Madsen et al., 2005; Goodwin et al., 2006; Nielsen et al., 2006; Lopez and Rink, 2007; Brooke et al., 2008a,b).

The Ilha Comprida barrier (southeastern Brazil) stands out due to its relatively well-preserved depositional landforms and sedimentary processes observed during the last decades, such as longshore growth, coastal progradation, coastal erosion, and dunefield formation. Thus, it can be considered an adequate setting to study changes in depositional dynamics of the southeastern Brazilian coast. In this work, optically stimulated luminescence (OSL) dating was used to evaluate chronologically the deposition and erosion of wave and eolian landforms (beach ridges, foredunes and blowouts) as well as to calculate rates of sediment deposition and coastal progradation. A detailed chronology of depositional and erosional events in the Ilha Comprida barrier during the last 1700 years is presented. This chronological framework was used as a basis to analyze the Late Holocene sedimentary dynamics of the barrier under physiography, relative sea level and climate changes in a subtropical coastal zone of the South Atlantic.

2. Regional setting

2.1. The Ilha Comprida barrier

The Ilha Comprida barrier is located on the southern coast of São Paulo State, in the southeast of Brazil (Fig. 1). The 63.5 km long (direction SW-NE) and 0.6–5 km wide barrier is situated seaward of the Cananéia-Iguape lagoon system (Tessler, 1982) and is bordered by the Cananéia and Icapara inlets. It is separated from the adjacent coastal zones by the Icapara Hill at the northern end, and by the Ilha do Cardoso Hill at the southern end. The barrier consists of sandy sediments, with the exception of a small hill (42 m high and less than 1 km large) of alkaline intrusive rocks in the southern part. Ilha Comprida is a coastal sand barrier formed by multiple coast-parallel beach and foredune ridges. It is a prograded barrier (sensu Roy et al., 1994) but it also can be considered a barrier island in a geomorphic sense (Reinson, 1979) because it is separated from the mainland by a lagoon.

The Ilha Comprida barrier was formed during the Late Quaternary (Suguio and Martin, 1978a; Giannini et al., 2003a; Guedes, 2003) by the deposition of sandy sediments in a wave-dominated coastal system. This barrier has been object of many geological studies since the middle of the 20th century (Geobrás, 1966; Suguio and Martin, 1978a; Tessler, 1988; Giannini et al., 2003a; Guedes, 2003). Nevertheless, many aspects of the chronology and evolution of this coastal zone remain to be clarified. ^{14}C dating of a wood trunk lying below sandy sediments of the innermost portion of the

barrier resulted in an age of 5308–4877 cal years BP (Giannini et al., 2003a). However, previous luminescence dating efforts of sediment samples distributed over the Ilha Comprida barrier showed many Late Pleistocene ages (Suguio et al., 1999, 2003; Guedes, 2003), which included ages contemporaneous to the Last Glacial Maximum (low relative sea level). These luminescence ages are inconsistent with the cited ^{14}C age (Guedes, 2003) as well as with relative sea level data for the Brazilian coast (Corrêa, 1996; Angulo et al., 2006). Therefore, these previous luminescence ages were not considered in this paper.

2.2. Climate, wind, wave, tides and fluvial input

The dominant climate in the Ilha Comprida coastal zone is wet subtropical with warm summers (IBGE, 1992). Meteorological data recorded near Ilha Comprida (Cananéia and Iguape) during the period from 1895 to 1990 indicate a mean air humidity greater than 70%, a mean annual precipitation of 1583 mm and a mean annual temperature of 21.1 °C (Geobrás, 1966; IPCC-DCC, 2000). The precipitation is well distributed throughout the year, with a slight increase during the summer. This coastal zone is situated in the middle of the South Atlantic Convergence Zone (SACZ), which separates the areas affected by Equatorial (Amazon basin source) and Tropical air masses to the north, and the areas affected by Polar air masses, to the south (Satyamurti et al., 1998). This belt determines the average northernmost extent of cold fronts formed by the encounter of Tropical Atlantic and Polar air masses. The Tropical Atlantic air mass is related to the NE trade winds while the Polar air mass migrates northward stimulating SE–S winds (Nimer, 1989; Nogués-Paegle and Mo, 1997). Changes in meteorological conditions like the formation of storm surges and increasing wind velocity are generally associated with the formation and northward advance of cold fronts (Satyamurti et al., 1998). The strongest and more frequent winds blow from the S and SE (mean velocity of 4.5 m/s) favored by the activity of cold fronts. Meteorological data (from 1990 to 1999) indicate that the cold fronts are more frequent and intense during the winter (Seluchi and Marengo, 2000; Rodrigues et al., 2004). Two swell wave systems act in the Ilha Comprida coast. The E and NE swell is associated with trade winds while the S and SE swell is related to cold fronts (Tessler, 1988). The wave heights (90%) range from 0.5 to 2.0 m, with 50% between 1 and 1.5 m (Geobrás, 1966; CTH-USP, 1973). The mean wave period during the action of SE winds is 8 ± 1 s (Geobrás, 1966). These two wave systems are responsible for alongshore transport systems with opposite directions but with a net predominance of NE transport as evidenced by the deviation of small tidal inlets and patterns in spatial variation of grain size and heavy minerals (Tessler, 1988; Giannini et al., 2008). The tides can be classified as semidiurnal with a mean astronomical range of 0.6 m (microtidal) measured at Cananéia Station (Harari et al., 2004).

A drainage system with an area of approximately 25,400 km^2 is present in the western mainland of the Ilha Comprida coastal zone. The Ribeira de Iguape River basin comprises more than 90% of this drainage system. Its main channel has a mean slope of 0.00059 m/m and an annual mean water flow of 375 m^3/s at its mouth (DAEE, 1998). The natural channel of the Ribeira de Iguape River reaches the Atlantic Ocean at the north of the Icapara Hill. An artificial channel (Valo Grande channel) was opened in 1852 to connect the lower Ribeira de Iguape River with the lagoon at the northern extremity of the Ilha Comprida barrier. It is estimated that 75% of today's sediment load transported by the Ribeira de Iguape River reaches the lagoon through the Valo Grande channel (Pisetta, 2006). The fluvial sediment input reaching the ocean is dominated by silt and clay but the content of sand increases during ebb tides. The sand of the middle Ribeira de Iguape River basin is relatively immature, with high content of lithic fragments (22–25%), feldspar (3–8%) and unstable heavy minerals (57–60%, within the heavy minerals of the very fine sand fraction) (De Maman, 2006). This composition is greatly different from the sands of the foreshore and active foredunes of the Ilha Comprida barrier, which are quartz rich and present relatively low content of unstable heavy minerals (11–24%) (Nascimento, 2006). These mineralogical differences suggest a minor contribution of sand directly derived from the Ribeira de Iguape River basin for the Ilha Comprida barrier building.

2.3. Barrier geomorphology

According to Nascimento (2006), the Ilha Comprida barrier beach is formed by well-sorted fine sand. It shows a wide swash zone (average of 75 m) and low slope (average of 0.67°). It has been classified as a dissipative beach (Stage 1 of Wright and Short, 1984). The Ilha Comprida barrier is formed by alignments of beach ridges, foredunes and blowouts. Sets of beach ridges dominate the barrier. Foredunes and blowouts occur only in the seaward portion of the barrier (up to 900 m from the present coastline). Parabolic dunes and a transgressive dunefield (with approximately 1 km^2) are present on the northeast end of the barrier. In this paper, "beach ridge" is considered as a marine deposit formed by wave action (Hesp et al., 2005): "*swash aligned, swash and storm wave built deposits or ridges.*" (Hesp, 1999). "Foredune" is "*typically the foremost vegetated sand dune formed on the backshore zone of beaches by aeolian sand deposition within vegetation. They are generally shore-parallel, vegetated, ramps, terraces and convex ridges separated by concave swales*" (Hesp, 1999). "Blowout" is a "*saucer-, cup- or trough-shaped depression or hollow formed by wind erosion on a preexisting deposit.*" (Hesp, 2002).

The seaward portion of the barrier comprises sets of active and stabilized foredunes with variable height. Active ridges of incipient (maximum height of 2.9 m) and established (maximum height of 3.6 m) foredunes, in the shape of ridge (main shape), terrace, or ramp, occur along the entire coastline. The incipient foredunes with terrace shape are situated near the tidal inlets at both ends of the barrier. The ramps of incipient foredunes are encroached on cliffs on established or relictic foredunes or beach ridges, mainly in the southwest portion of the barrier (10–26 km from the SW extremity). Stabilized foredunes are present as ridges defined by the contrast in vegetation type and density as well as by their great height in comparison with active foredunes and with beach ridges. In the seaward portion of the barrier, the stabilized foredunes are differentiated from the active foredunes by their arboreal vegetation, higher degree of cementation, presence of paleosols, lateral discontinuity and greater height (Fig. 2). The number of foredune ridges visible in aerial photos varies from two to six and their lateral continuity is interrupted by the presence of blowouts (Guedes, 2003; Giannini et al., 2003a, 2008). The direction of the stabilized foredunes differs from the present coastline and active foredunes. Wave-erosion scarps occur in stabilized foredunes located at the coastline (Nascimento, 2006). Blowouts with NNW depositional lobes occur attached or separated from foredune ridges. Attached and laterally coalesced blowouts are responsible for the sinuosity of the crests of foredunes. Locally, non-attached blowouts can evolve windward to parabolic dunes and barchanoid chains of a transgressive dunefield migrating to NNW at the northern portion of the barrier (Giannini et al., 2008). The main depositional landforms of the seaward portion of the Ilha Comprida barrier can be viewed in Fig. 2.

2.4. Late Quaternary relative sea level changes

The Late Quaternary relative sea level (RSL) changes on the Brazilian coast fit with the global glacioeustatic changes. Two phases of RSL rise or highstand have been identified during the Late

Fig. 2. Ilha Comprida barrier (A), sets of low foredunes (B), up to 15 m high reactivated blowouts (C) and blowout alignment with higher relief landward of active foredunes (D).

Pleistocene and Holocene. The oldest RSL rise is linked to the Last Interglacial period and reached 8 ± 2 m above the present sea level at around 120 ka BP (Martin et al., 1988). This RSL rise and highstand was followed by an RSL fall, which reached approximately 130 m below the present level during the Last Glacial Maximum (LGM), at around 18 ka BP (Corrêa, 1996). The youngest RSL rise started after the Last Glacial period, giving origin to the present highstand (Van Andel and Laborel, 1964; Suguio et al., 1985; Angulo et al., 2006). This post-LGM RSL rise comprised three stillstand phases at approximately 11, 9 and 8 ka BP (Kowsmann and Costa, 1979; Corrêa, 1996). Suguio et al. (1985) proposed that the maximum Holocene RSL at the Ilha Comprida region was less than 4 m above the present level and occurred at around 5.1 ka BP. Using vermetid fossil shells as RSL indicators, Angulo and Lessa (1997) and Angulo et al. (1999) recognized a gentle decline of sea level from around 5.0 ka BP to the present in the southeastern and southern Brazilian coast. Vermetid shell data for the coasts of Rio de Janeiro, São Paulo and Paraná states, compiled and reinterpreted by Angulo et al. (2006), confirmed the pattern of RSL fall from 5.0 ka BP to present (Fig. 3). These data are considered to be representative of the RSL changes in the Ilha Comprida coastal zone. As pointed out by Angulo et al. (2006), the Middle Holocene RSL maximum and the following RSL fall determined through vermetid data are in good agreement with the global eustatic curve predicted by the model of Milne et al. (1999).

According to Suguio and Martin (1978a), the Ilha Comprida barrier comprises sediments deposited during the last Pleistocene RSL highstand (approximately 8 m above the present RSL at 120 ka A.P.), which served as a nucleus for the deposition of Holocene sediments after the LGM. However, Guedes (2003) and Giannini et al. (2003a,b, 2008) proposed that the Ilha Comprida barrier was deposited entirely during the Holocene RSL highstand without Pleistocene deposition.

3. Methods

3.1. Sampling

Twenty-seven sediment samples were collected in outcrops or along profiles across the foredunes and blowouts during May of 2005 (Fig. 4). The profile topography was determined using GPS and barometer–altimeter. The samples were collected along vertical sections, in the outcrops, and in pits at the top of the foredunes, blowouts and beach ridges, in the profiles. This procedure allowed evaluating the consistency of OSL ages through comparison between adjacent ages (ages must decrease from base to top in outcrops and seaward in profiles). The samples for

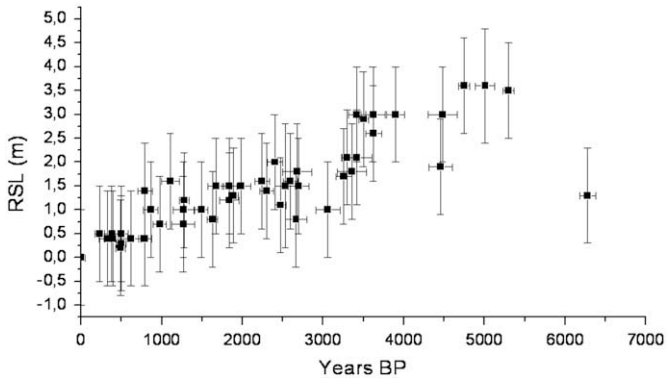

Fig. 3. Variation of relative sea level based on vermetid shell data collected at the coasts of Rio de Janeiro, São Paulo and Paraná states. Data compiled and reinterpreted by Angulo et al. (2006) from Delibrias and Laborel (1969), Martin and Suguio (1978a, 1989), Suguio and Martin (1978b), Flexor et al. (1979), Martin et al. (1979, 1979/1980, 1996, 1997), Angulo (1994), Angulo et al. (2002).

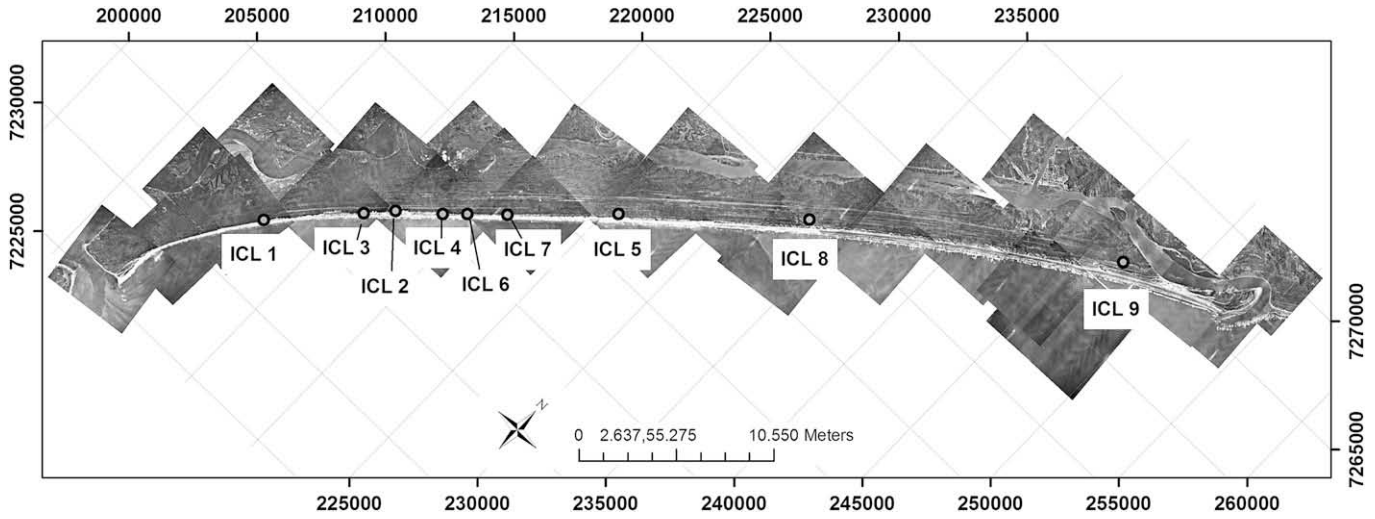

Fig. 4. Dating sites of the Ilha Comprida barrier. The samples were collected in depositional forms of the seaward portion of the barrier. The mosaic comprises aerial pictures of 1962.

determination of radiation doses were collected by pushing opaque PVC tubes into the center of a sedimentologically homogeneous area with at least 30 cm radius (range of gamma radiation in soil). This procedure ensured that the material collected separately for dose rate measurements was representative for the total relevant sediment volume.

3.2. Optically stimulated luminescence (OSL) dating procedures

In OSL dating, the time elapsed since deposition of a sediment layer is determined from the radiation dose accumulated in minerals since the last sunlight exposure, and the dose rate due to naturally occurring radioactive nuclides and cosmic radiation:

$$\text{Age[a]} = \frac{\text{Equivalent dose[Gy]}}{\text{Dose rate[Gy/a]}}$$

Radiation exposure can be measured by stimulating the sample with light of one wavelength and monitoring the luminescence at another wavelength (OSL). The intensity of the OSL is a function of the absorbed natural radiation dose. Detailed discussions of luminescence dating methods including equivalent dose and dose rate determination can be found in books by Aitken (1998) and Bøtter-Jensen et al. (2003), and a review by Lian and Roberts (2006).

The samples consist mainly of quartz. Therefore, 120–150 μm quartz separates were prepared under red light by treatment with H_2O_2 27%, HCl 3.75%, HF 48–51% for 40 min, and subsequent density separation with sodium polytungstate solution (density 2.75 g/cm^3 and 2.62 g/cm^3).

The OSL measurements were carried out with two automated Risø DA-15 TL/OSL systems, Risø National Laboratory, in the Radiation Dosimetry Laboratory at Oklahoma State University (Stillwater). The readers are equipped with bialkali PM tubes (Thorn EMI 9635QB) and Hoya U-340 filters (290–370 nm). The built-in ^{90}Sr/^{90}Y beta sources give dose rates of 104 ± 3.9 mGy/s and 94.9 ± 2.9 mGy/s, respectively. Optical stimulation was carried out with blue LEDs (470 nm), delivering 45 mW/cm^2 to the sample. The heating rate used was 5 °C/s.

The Single-Aliquot Regenerative-Dose procedure (SAR) described in Table 1 was applied as proposed by Murray and Wintle (2000) and Wintle and Murray (2006). Suitable preheat temperatures were determined with a plateau test, using samples ICL1, ICL4A and ICL9A which are representative of the whole investigated geographical area. 220 °C was selected as the common preheat temperature for all samples. The OSL signal was obtained by integrating the first two seconds of the shine down curve while the background was determined by integrating the last 10 s. For each sample 24 aliquots were measured. "Reliable" aliquots for dose determination were chosen following the tests proposed by Murray and Wintle (2000) and Wintle and Murray (2006), including recycling ratio, recovery of a known dose, recuperation, and IR depletion of the OSL signal. Only few aliquots were sorted out due to a recuperation signal larger than 5% of the natural signal.

The equivalent dose was determined by linear fitting of the dose–response function. For very young samples, with doses smaller than the lowest dose applicable with the beta sources, a linear trend was assumed also for the dose response between 0 and 1000 mGy (Fig. 5). For each sample, the final dose was determined from the weighted mean of all reliable aliquots.

The concentrations of ^{40}K, uranium and thorium were determined with a shielded high purity germanium detector (HPGe). Spectra of empty containers were acquired for background evaluation. Beta and gamma dose rates were calculated using the conversion factors given by Adamiec and Aitken (1998). The contribution of cosmic radiation to the dose rate was calculated as described by Barbouti and Rastin (1983) and Prescott and Stephan (1982) using latitude, longitude, altitude, depth, and density of the

Table 1
The SAR procedure used for equivalent-dose determination

1. Regeneration dose (D_i)
2. Preheat at 220 °C for 10 s
3. Measure OSL at 125 °C for 80 s (R_i)
4. Test dose (TD_i)
5. Preheat at 220 °C for 10 s
6. Measure OSL at 125 °C for 80 s (T_i)
7. Repeat steps 1–6 for a range of regeneration doses
8. Find sensitivity-corrected OSL $L_i = R_i/T_i$
cycle 1: $D_1 = 0$
cycle 2–5: dose–response with regeneration doses D_2, D_3, D_4, D_5
cycle 6–7: repeat doses with $D_3 < D_6 < D_4$ and $D_7 = D_2$
cycle 8: $D_8 = 0$
cycle 9: dose $D_9 = D_6$ with additional IR stimulation at 60 °C for 100 s between steps 1 and 2

The irradiation times were $TD_i = 2$ s, $D_2 = 10$ s, $D_3 = 12$ s, $D_4 = 14$ s, $D_5 = 16$ s, $D_6 = 13$ s, using two ^{90}Sr/^{90}Y beta sources with dose rates of 104 ± 3.9 mGy/s and 94.9 ± 2.9 mGy/s, respectively.

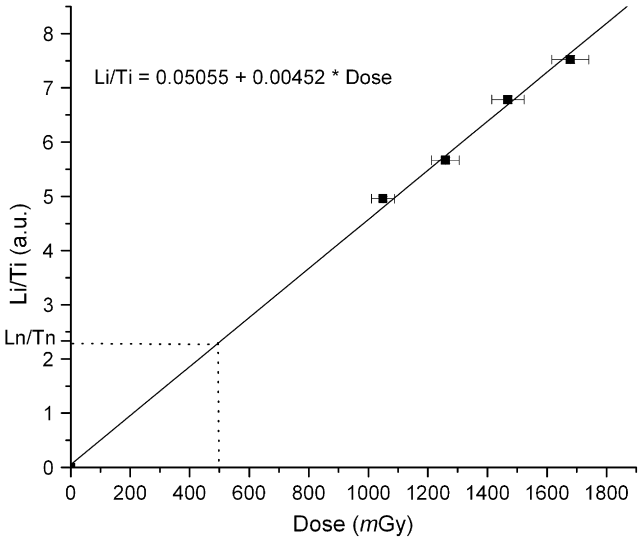

Fig. 5. Linear relation between known given radiation doses and corrected OSL signals (L_i/T_i) for one aliquot of sample ICL1. For this aliquot, the maximum errors of L_i/T_i and dose were 0.073 and 62 mGy, respectively. The natural radiation dose was determined using a linear dose–response function. The values of the natural signal ($L_n/T_n = 2.336 \pm 0.023$) and its respective dose are marked by the dotted lines.

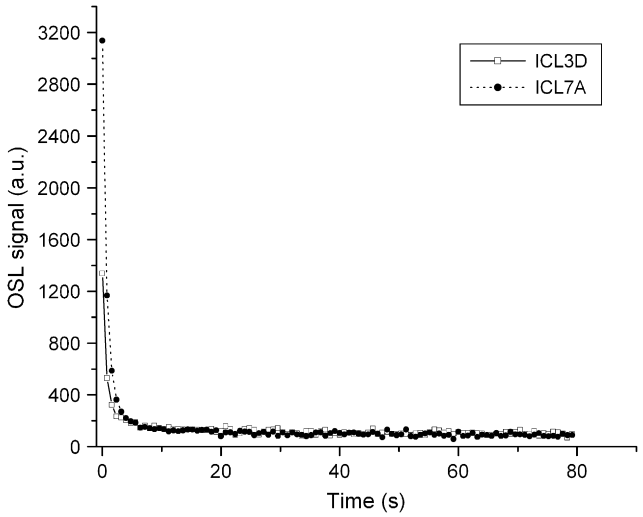

Fig. 6. OSL curves (natural OSL signals) of quartz aliquots of the samples ICL3D and ICL7A. Both samples presented radiation doses smaller than 100 mGy.

samples. A 10% uncertainty was assumed. The total error of the dose rate was calculated according the Gaussian law of error propagation.

4. Results

4.1. Dating results

The quartz grains extracted from the samples show a very high sensitivity which allowed good counting statistics even in the case of very low natural doses (Fig. 6). This is in agreement with the observation that sedimentary reworking can act as a natural luminescence sensitizer of quartz (Pietsch et al., 2008).

The dose distributions of all samples showed low variability and only one peak, indicating effective bleaching prior to deposition (Fig. 7).

These characteristics are compatible with the high content of quartz and high homogeneity and sedimentary reworking of the Ilha Comprida barrier sands. The samples were collected above the phreatic level, i.e. the water content ranged from 4 to 7% (weight percent). Table 2 shows the equivalent doses, dose rates and OSL ages determined for the Ilha Comprida samples.

The oldest and youngest OSL ages obtained were 1697 ± 159 years and 53 ± 8 years, respectively. The dating sites are shown in Fig. 4. These sites are described in detail in Figs. 8–12. The ages of all vertical profiles in outcrops decrease from base to top, while in the profiles across foredune and beach ridges the ages decrease seaward. These patterns are geologically consistent and confirm the suitability of the SAR procedure for the Ilha Comprida sands. The main differences between previous luminescence dating attempts with multiple aliquot methods (Suguio et al., 1999, 2003; Guedes, 2003), and the ages presented here are related to the natural accumulated radiation doses. This demonstrates the advantage of the SAR procedure in relation to multiple aliquot methods for dose determination.

4.2. Chronology of the Ilha Comprida barrier landforms

Only the seaward part ($\sim$1 km wide) of the Ilha Comprida barrier comprises eolian depositional landforms, which include stabilized and active foredunes, blowouts and a small ($\sim$1 km^2) transgressive dunefield. Based on the presence or not and type of the eolian landforms, the Ilha Comprida barrier can be divided seaward into three units (inner, middle and outer unit) identifiable on aerial photos by their depositional morphology (Fig. 8) (Guedes, 2003). The inner unit is formed by low sand ridges (up to 0.5 m high) interpreted as beach ridges. Its seaward limit marks the beginning of the zone of the eolian depositional landforms. The middle unit is formed by a belt of NNW blowouts up to 15 m high aligned alongshore. The NNW orientation of the blowout lobes indicates their development by cold front winds (SSE winds). Based on this alignment and blowout height, it is deduced that the blowouts were formed by the rupture of preexisting foredune ridges. The outer unit comprises a series of active (seaward) and stabilized foredunes with localized blowouts and a small transgressive dunefield migrating to NNW at the northern extremity of the barrier. This unit has variable width alongshore, allowing the formation of wave-erosion scarps in the blowouts of the middle unit in the central portion of the barrier. In this place, the blowouts of the middle unit are covered by a thin bed (up to 1 m thick) of cross stratified white sand which correlates to the outer unit and is separated from the main blowout lobe sand by paleosols or erosion surfaces (Fig. 9). Giannini et al. (2008) divided the eolian landforms of the Ilha Comprida barrier into three depositional units: (1) high paleodune ridges (up to 15 m high), with sinuosity attributed to old blowouts tens of meters long, (2) low stabilized foredune ridges (up to 3.5 m high), and (3) active foredune ridges, blowouts and dunefield. The middle unit defined here corresponds to their eolian unit 1, while the outer unit corresponds to their eolian units 2 and 3.

Three luminescence ages were obtained for the inner unit (Table 2). A sample collected approximately 1 m below the crest of a beach ridge adjacent to a blowout lobe of the middle unit, dated to 1004 ± 88 years (ICL1, Fig. 10). The other two samples of the inner unit consisted of massive well-sorted fine sand and were collected below paleosol horizons lying beneath the deposits of blowout lobes of the middle unit. They dated to 1186 ± 98 (ICL2A) and 1697 ± 159 years (ICL3A). Guedes (2003) and Giannini et al. (2003a, 2008) dated an in situ wood trunk from a muddy facies below a set of fine sand with plan parallel stratification (foreshore sediments) outcropping at the lagoon side of the Ilha Comprida barrier. The obtained radiocarbon age of 4530 ± 70 years BP (5308–4877 cal years BP) can be interpreted as an approximate age for the beginning of coastal progradation and as the maximum age of the inner unit in the southern portion of the barrier.

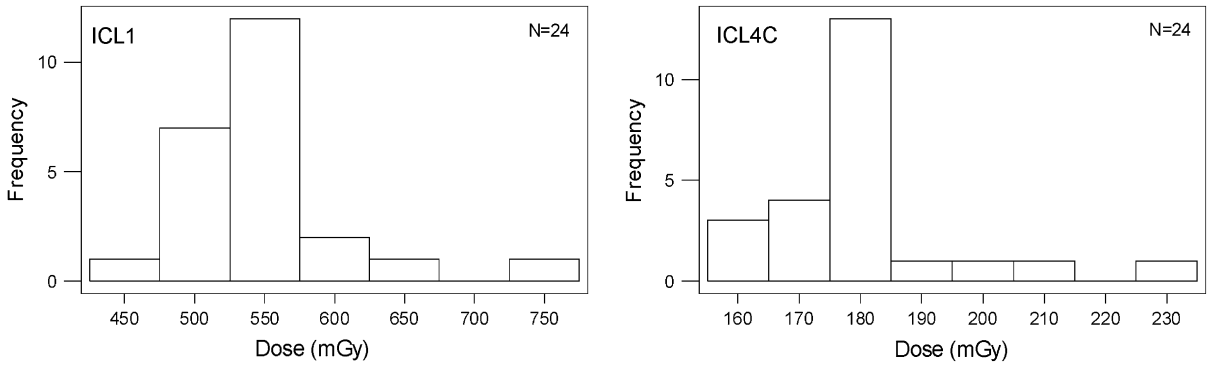

Fig. 7. Frequency distributions of equivalent radiation doses measured in aliquots of samples ICL1 and ICL4C.

The age range of the blowout lobes of the middle unit is 575 ± 47 (ICL6A) to 172 ± 18 years (ICL4C) (Figs. 8–12). The OSL ages showed that this blowout formation is well restricted in time. The most active period occurred about 300–200 years ago (relative to the year of 2005).

The outer unit comprises foredunes with ages less than 108 ± 10 years (ICL1B, sand from the crest of the foredune adjacent to the stabilized blowout lobe). In the southern portion of the barrier, the sands capping the blowouts of the middle unit (located at the coastline) gave ages between 53 ± 8 and 74 ± 16 years. Thus, the reaching of old blowouts by the locally transgressive coastline allowed their recent covering by young eolian sands.

The deposits corresponding to the three geomorphological units can be found horizontally (Figs. 10 and 11) as well as vertically stacked. The vertical stacking is possible because the blowout lobes of the middle unit advanced locally on the beach ridges of the inner unit and the top of the blowouts of the middle unit can be covered by young eolian deposits of the outer unit when they are near the present coastline. In outcrops, the deposits of these three units are separated by paleosol horizons, which confirm the depositional hiatus between them, as it is expected due to differences in sand ridge orientation.

The beach ridge ages of the inner unit indicate an end of coastal progradation without significant eolian deposition at least 1004 ± 88 years ago. Blowout formation in the middle unit is interpreted as a short-time event because of the relative synchronicity of the blowout lobes alongshore (see sections ICL1–ICL9 in Figs. 8–11). These blowouts would be related to wave-erosion of preexisting foredunes due to the following characteristics: (i) blowouts distributed alongshore (approximately 63 km of coastline) are aligned differently from the older sets of beach ridges in the inner unit; (ii) blowouts of similar ages overlap beach ridges of different ages, indicating the erosion of beach ridges before blowout initiation. The outer unit comprises sets of low foredune ridges, indicating a new phase of coastal progradation. The four adjacent foredune ridges of the profile ICL1 (distributed along a distance of only 25 m) had the same age within their error limits, suggesting that coastal progradation was relatively fast (below the time resolution of OSL dating) during recent periods.

The inner, middle and outer units represent the geomorphological evolution of the Ilha Comprida barrier, which stands out due the development of eolian landforms during the last 600 years. This evolution is summarized by: (1) an old phase of coastal progradation without significant eolian activity (inner unit), (2) a phase of coastal erosion with important eolian deposition, represented by high foredunes and blowouts (middle unit), and (3) a young phase of fast and variable coastal progradation with the development of low foredunes (outer unit). The three phases of coastal evolution are well exemplified by the depositional landforms and ages of the profile ICL1 (Fig. 11).

4.3. Deposition and progradation rates

Luminescence ages obtained in vertical profiles made it possible to calculate rates of sediment deposition. Sediment samples from the same foredune or blowout lobe sets of cross stratification presented no age differences. Significant age differences were observed only between sand facies separated by paleosol horizons or erosion surfaces (Fig. 12). Therefore, foredune ridges and blowouts appear to result from relatively fast depositional events characterized by short-time periods of deposition separated by relative long time periods of stabilization and soil formation.

Beach ridges and foredune ridges are indicators of past shoreline positions (Otvos, 2000). Thus, by dating profiles across beach and foredune ridges, rates of coastal progradation can be calculated. The inner and outer units presented different progradation rates (Table 3). Based on the radiocarbon age of 5308–4877 cal years BP (Guedes, 2003; Giannini et al., 2003a, 2008), representative of the oldest beach ridge, a progradation rate of 0.71–0.82 m/year was calculated for the inner unit. Ridge crests with different orientation within the inner unit indicate that its progradation was not continuous. The outer unit presented higher progradation rates. However, these rates were highly variable alongshore: 0.86–1.04 m/year (at profile ICL1) and 1.86–2.23 m/year (at profile ICL8). It should be noted that the foredune ridges of the outer unit are not continuous alongshore, and are absent in the south-central portion of the barrier (sites ICL2, ICL3 and ICL4). This unit becomes wider from this zone to south and north and its progradation rates increase northward.

5. Discussion

5.1. The Ilha Comprida barrier progradation rates: comparison with other sand barriers

Barrier progradation is controlled by the relation between sediment supply and accommodation space, and by the variation of these two variables in space and time. On a thousand to hundred years timescale, sediment supply to coastal systems is highly dependent on climate. The climate controls sediment input from rivers and sediment transport by wind and waves. However, changes in coastal physiography can modify pathways of alongshore transport and the input/output balance of sediments in a coastal sector. The seabed slope influences the onshore and offshore sediment transport. Gently sloping surfaces favor the onshore sand deposition and coastal progradation (Roy et al., 1994). Variation in embayment geometry and depth profile produces spatial changes in accommodation space. Thus, the barrier advance on deeper zones will reduce the progradation rate.

Shifts in the progradation rate are correlated with changes in the Ilha Comprida barrier geomorphology. The inner unit showed

Table 2
Equivalent natural radiation doses, effective radiation dose rates and OSL ages determined for the Ilha Comprida samples

Sample	UTM (LON//LAT)	Distance from coastline (m)	Elevation above RSL (m)	Landform	Unit	Dose (mGy)	Gamma dose rate (mGy/year)	Beta dose rate (mGy/year)	Cosmic dose rate (mGy/year)	Total dose rate (mGy/year)	Age (years)
ICL1	212004// 7233758	206	3.2 ± 0.1	BR	Inner	550 ± 35	0.170 ± 0.019	0.218 ± 0.027	0.1588 ± 0.0079	0.547 ± 0.033	1004 ± 88
ICL1A	212043// 7233737	162	6.2 ± 0.1	BT	Middle	363 ± 23	0.477 ± 0.053	0.476 ± 0.057	0.1628 ± 0.0081	1.116 ± 0.078	325 ± 31
ICL1B	212098// 7233711	102	3.2 ± 0.1	FD	Outer	82 ± 6	0.303 ± 0.032	0.300 ± 0.035	0.1628 ± 0.0081	0.765 ± 0.049	108 ± 10
ICL1C	212100// 7233714	101	3.2 ± 0.1	FD	Outer	51 ± 5	0.154 ± 0.016	0.211 ± 0.025	0.1627 ± 0.0081	0.528 ± 0.031	97 ± 11
ICL1D	212104// 7233703	91	3.2 ± 0.1	FD	Outer	66 ± 5	0.225 ± 0.024	0.334 ± 0.039	0.1627 ± 0.0081	0.722 ± 0.046	91 ± 9
ICL1E	212113// 7233690	77	3.2 ± 0.1	FD	Outer	47 ± 5	0.163 ± 0.018	0.200 ± 0.025	0.1628 ± 0.0081	0.526 ± 0.032	89 ± 11
ICL2A	216774// 7239078	140	2.0 ± 0.1	BR	Inner	469 ± 26	0.125 ± 0.014	0.155 ± 0.019	0.1145 ± 0.0057	0.395 ± 0.024	1186 ± 98
ICL2B	216774// 7239078	140	3.5 ± 0.1	BT	Middle	73 ± 9	0.109 ± 0.012	0.153 ± 0.019	0.1351 ± 0.0068	0.397 ± 0.023	184 ± 25
ICL3A	215638// 7237798	70	3.0 ± 0.1	BR	Inner	804 ± 55	0.145 ± 0.016	0.206 ± 0.025	0.1223 ± 0.0061	0.474 ± 0.030	1697 ± 159
ICL3B	215638// 7237798	70	3.7 ± 0.1	BT	Middle	289 ± 42	0.298 ± 0.033	0.355 ± 0.043	0.1285 ± 0.0064	0.782 ± 0.054	370 ± 60
ICL3C	215638// 7237798	70	4.8 ± 0.1	BT	Middle	256 ± 15	0.277 ± 0.030	0.295 ± 0.035	0.1384 ± 0.0069	0.710 ± 0.046	360 ± 31
ICL3D	215638// 7237798	70	6.2 ± 0.1	ES-BT	Outer	40 ± 5	0.281 ± 0.030	0.315 ± 0.037	0.1519 ± 0.0076	0.748 ± 0.049	53 ± 8
ICL4A	218735// 7240727	0	0.0 ± 0.1	BR	Middle	326 ± 13	0.240 ± 0.025	0.257 ± 0.028	0.1305 ± 0.0065	0.627 ± 0.039	520 ± 38
ICL4B	218735// 7240727	0	1.1 ± 0.1	BT	Middle	164 ± 11	0.415 ± 0.046	0.397 ± 0.048	0.1407 ± 0.0070	0.953 ± 0.067	172 ± 17
ICL4C	218735// 7240727	0	1.7 ± 0.1	BT	Middle	181 ± 14	0.465 ± 0.051	0.439 ± 0.052	0.1461 ± 0.0073	1.050 ± 0.073	172 ± 18
ICL4D	218735// 7240727	0	2.4 ± 0.1	ES-BT	Outer	40 ± 5	0.251 ± 0.028	0.266 ± 0.032	0.1533 ± 0.0077	0.663 ± 0.043	60 ± 8
ICL5	225602// 7247346	250	> 2.0 ± 0.1	BT	Middle	232 ± 18	0.124 ± 0.014	0.204 ± 0.025	0.1497 ± 0.0075	0.475 ± 0.029	489 ± 48
ICL6A	219716// 7241654	0	2.0 ± 0.1	BT	Middle	298 ± 16	0.172 ± 0.020	0.199 ± 0.025	0.1145 ± 0.0057	0.518 ± 0.032	575 ± 47
ICL6B	219716// 7241654	0	4.7 ± 0.1	ES-BT	Outer	66 ± 4	0.234 ± 0.027	0.250 ± 0.031	0.1374 ± 0.0069	0.630 ± 0.042	105 ± 9
ICL7A	221301/ 7243121	0	3.1 ± 0.1	BT	Middle	84 ± 5	0.119 ± 0.013	0.181 ± 0.022	0.1507 ± 0.0075	0.447 ± 0.027	188 ± 16
ICL7B	221301// 7243121	0	4.0 ± 0.1	ES-BT	Outer	43 ± 9	0.199 ± 0.022	0.238 ± 0.029	0.1604 ± 0.0080	0.583 ± 0.038	74 ± 16
ICL8A	233244// 7254314	565	7.0 ± 0.1	BT	Middle	156 ± 7	0.138 ± 0.015	0.277 ± 0.034	0.155 ± 0.0077	0.561 ± 0.038	278 ± 22
ICL8B	233244// 7254314	379	4.0 ± 0.1	FD	Middle	121 ± 7	0.183 ± 0.020	0.316 ± 0.038	0.1549 ± 0.0077	0.645 ± 0.044	187 ± 17
ICL8C	233244// 7254314	323	1.4 ± 0.1	FD	Outer	53 ± 6	0.160 ± 0.018	0.277 ± 0.033	0.1649 ± 0.0082	0.583 ± 0.039	91 ± 12
ICL9A	247089// 7264479	825	> 2.5 ± 0.1	BT	Middle	181 ± 9	0.144 ± 0.016	0.286 ± 0.034	0.1263 ± 0.0063	0.577 ± 0.038	313 ± 26
ICL9B	247089// 7264479	825	> 3.9 ± 0.1	BT	Middle	197 ± 8	0.220 ± 0.025	0.340 ± 0.041	0.1388 ± 0.0069	0.706 ± 0.048	279 ± 22
ICL9C	247089// 7264479	825	> 6 ± 0.1	BT	Middle	198 ± 15	0.317 ± 0.037	0.429 ± 0.051	0.1604 ± 0.0080	0.892 ± 0.064	222 ± 23

Samples with the same identification number belong to the same outcrop (vertical profiles) or profile across blowout, foredune and beach ridges. The last character is related to the position of the sample in the profile. A to E indicates bottom to top in vertical profiles and land to sea in profiles across beach ridges. The samples were classified regarding their sedimentary origin in: BR = beach ridges; FD = foredunes; BT = Blowouts; ES-BT = eolian sand covering blowouts. Distance from the coastline (0 m indicates outcrops at the coastline) and elevation (above RSL) of each sample are also presented.

progradation rates of 0.71–0.82 m/year. The middle unit originated in a period with pronounced coastal erosion. The outer unit presented higher and variable progradation rates (0.86–2.23 m/year). The progradation rates calculated for inner unit are net rates, which include periods of coastal erosion indicated by the truncation between beach ridges. Another point to consider is that the geomorphological units developed under different timescales. The outer unit comprises timescale from tens to a hundred years and the inner unit, timescale of a thousand (inner unit) years. This affects the comparison of their progradation rates due to the "paradox of sedimentation rate" (Sadler, 1981; Korvin, 1992), which denotes discrepancies between the rates of sedimentation determined for different timescales (the longer the time interval, the less is the sedimentation rate). In this way, the higher progradation rates of the outer unit can be attributed at least in part to its lower time interval.

Holocene coastal plains worldwide (data compiled from United States of America, Denmark, Spain, Australia, New Zealand and Argentina barriers) are dominated by a relative narrow range of progradation rates (Table 4). On a 100 years timescale (100–900 years), the first and third quartiles of the compiled progradation rates were 0.47 and 1.02 m/year, respectively. These values are slightly higher than the values determined on a 1000 years timescale (1000–6300): 0.34 and 1.00 m/year, respectively, for the first and third quartiles (Table 5). It should be pointed out that Australian barriers dominate the compiled data. The range of

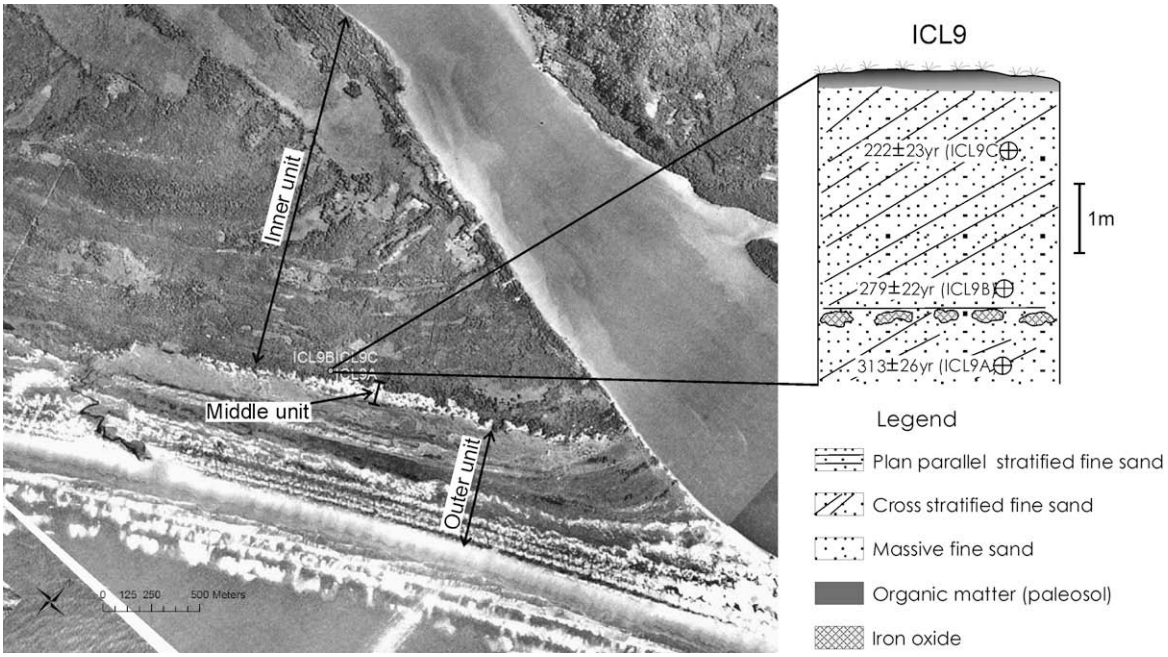

Fig. 8. Geomorphological units (outer, middle and inner) recognized in the Ilha Comprida barrier. The inner unit is formed by sets of well-vegetated beach ridges. The middle unit comprises a narrow zone of blowouts up to 15 m high. The ages obtained for the site ICL9 (outcrop in blowout) are shown in the picture. The outer unit is characterized by poorly vegetated sets of low foredunes. This unit still presents a small dunefield ($\sim 1\ km^2$) at the northernmost portion of the barrier. Aerial picture of 1962.

progradation rates of the Ilha Comprida barrier is similar to that of the Australian barriers (Table 5). The barriers of both settings share some characteristics, like the development at a tectonically stable sandy coast, far from the influence of glacial isostasy and with similar Holocene relative sea level changes (2–3 m higher than the present level at the Middle Holocene, followed by a slow decrease). However, the coastal settings are significantly different with regard to climate.

The relative narrow range of progradation rates observed in Holocene barriers of distinct climatic and physiographic contexts suggests that the record of short-time variations in progradation are limited by low order changes in the accommodation space. For Holocene coastal systems, the accommodation space increased globally in an approximately synchronous manner due to the post-LGM sea level rise. Thus, the progradation rates of Holocene barriers would be modulated by the post-LGM eustatic rise. In this case, the great variation of barrier width worldwide would result not only by changes in progradation rates but also by the time elapsed since the beginning of the progradation. This low order control would minimize the effect of local and short-time events, with higher spatial and temporal variability. This is in agreement with the "Coastal Tract" concept (Cowell et al., 2003a, 2003b), which argues that short-time processes (sub-decades) cannot describe long-term coastal evolution (centennial to millennial timescale). Thus, only major and persistent climatic or physiographic shifts, which have lower variability, would produce detectable changes in barrier progradation rates.

5.2. Controls on the development of blowouts and foredunes of the Ilha Comprida barrier

The development of foredunes depends on sand supply, type and degree of vegetation cover, frequency and magnitude of wind and waves, beach morphodynamics, sea level, and coastline stability (Hesp, 2002). According to Hesp (2002), blowouts can be initiated by wave-erosion along the seaward face of foredunes, topographic acceleration of airflow over the foredune crest and/or vegetation variation in space and time linked with climate change or human activities. Foredunes and blowouts occupy only the seaward portion of the Ilha Comprida barrier. These eolian sediments were deposited approximately during the last 600 years (old blowout lobe of the middle unit with age of 575 ± 47 years), suggesting an important shift in the barrier sedimentary evolution. Bristow and Pucillo (2006) and Brooke et al. (2008a) have observed a link between reduction in progradation rates and foredune building in some Australian barriers. As discussed, progradation rates varied between the inner (0.71–0.82 m/year), middle (coastal erosion and stability) and outer (0.86–2.23 m/year) units. These changes in progradation rates reflect shifts in the morphodynamics of the Ilha Comprida barrier building. The first shift corresponds to an interruption of the progradation and development of high foredunes and blowouts. This shift marks the transition from a beach ridges progradational barrier to a foredune/blowouted ridges barrier. The second shift is characterized by higher and variable progradation rates, but under conditions favorable to the formation of low foredunes and a small transgressive dunefield.

Progradation rate is controlled by the balance between sediment supply and accommodation space. The increase in accommodation space due to relative sea level rise can induce wave erosion and stop or reduce the coastal progradation. This would favor the development of the high foredunes and blowouts of the middle unit. However, the vermetid shell data acquired at the coasts of Rio de Janeiro, São Paulo and Paraná states show a gradual relative sea level fall with approximately constant rate from 5.0 ka years BP to present (Fig. 3). Therefore, there are no Holocene changes in the relative sea level related to variations in the progradation rates of the Ilha Comprida barrier.

Coastal progradation is also influenced by seabed geometry because higher slopes produce deeper zones, which require more sediment for coastal plain growth (Roy et al., 1994). Depth variation can be viewed as a physiographic change in the accommodation space. Based on this mechanism, the reduction in the progradation rates of the Ilha Comprida barrier during the development of the middle unit would be related to the seaward barrier growth on

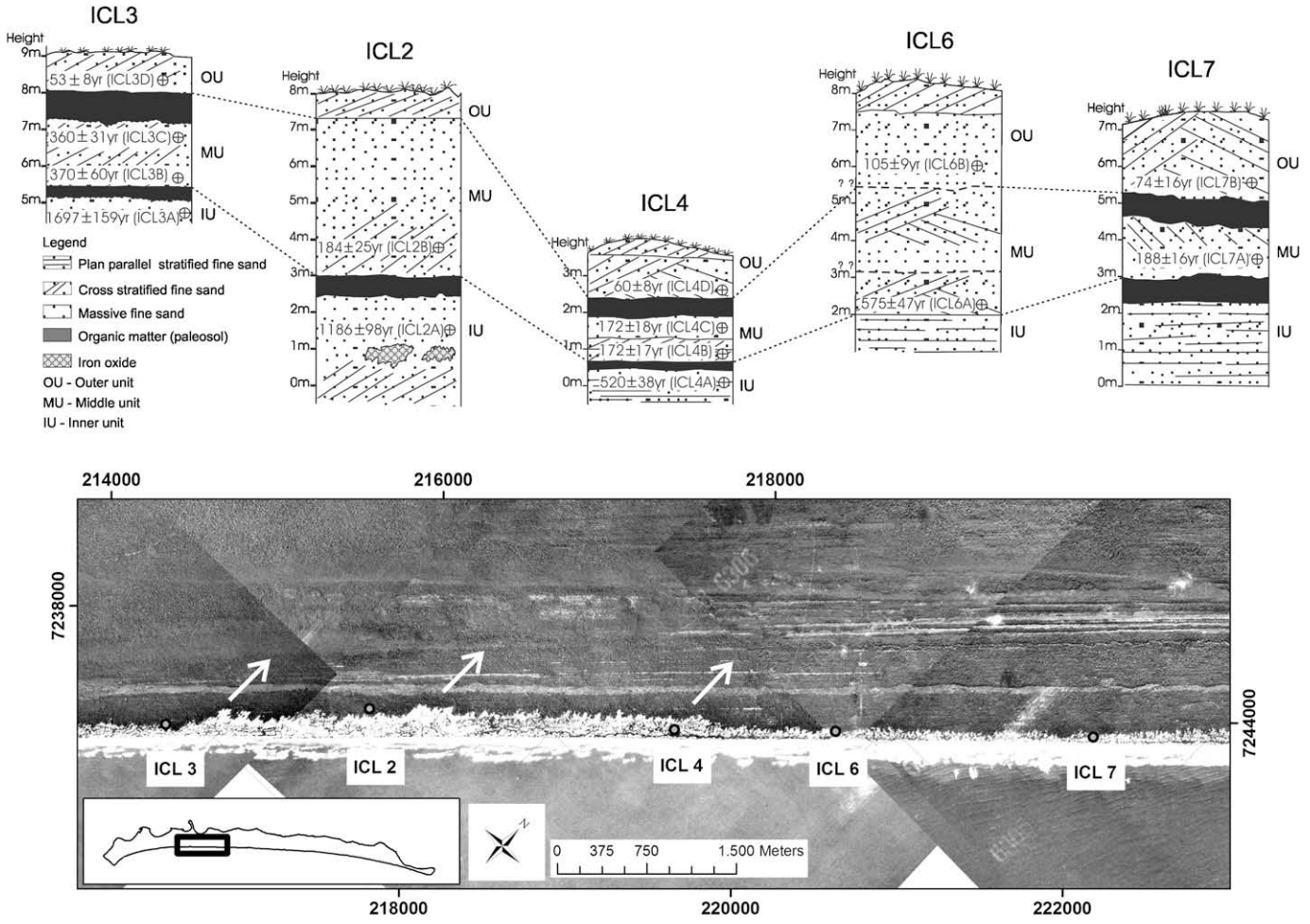

Fig. 9. Columnar sections and luminescence ages obtained in outcrops of sites ICL2, ICL3, ICL4, ICL6 and ICL7. In this zone, the blowouts of the middle unit form erosion scarps at the coastline, favoring their reactivation or covering by young eolian sands of the outer unit. Blowout lobe sands of the middle unit are separated from beach ridge sands of the inner unit by paleosol horizons or erosion surfaces. The white arrows indicate the orientation of blowout lobes.

a higher slope zone. Nevertheless, the relatively narrow width of the middle unit, which is followed by sets of foredune ridges developed under higher progradation rates, refutes this hypothesis. Coastal progradation also depends on coastline length. Longer coastlines need more sediment to prograd. However, the Ilha Comprida barrier coastline reached more than 90% of its present length already during the development of the inner unit (Giannini et al., 2008).

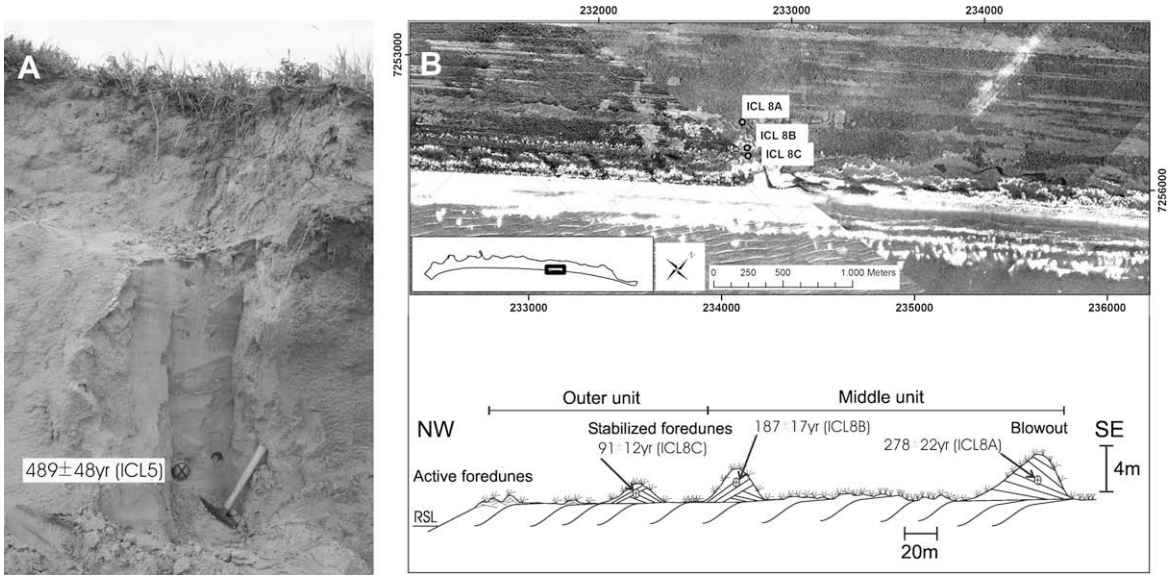

Fig. 10. Luminescence ages of the blowout sampled at site ICL5 (A) and of active and stabilized foredunes (outer and middle units) and blowout (middle unit) of the profile ICL8 (B).

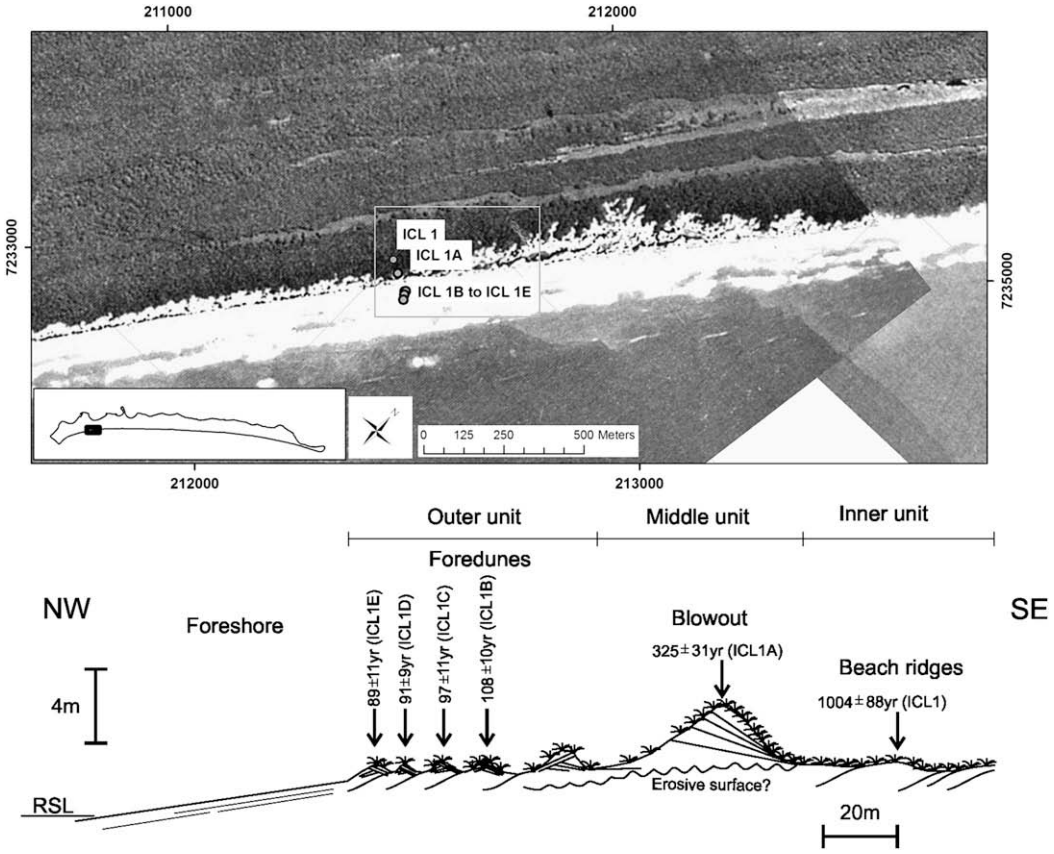

Fig. 11. Inner, middle and outer units in a profile across ridge orientation at site ICL1. The young phase of progradation (sets of low foredune ridges of the outer unit) began after the episode of high foredune and blowout formation (middle unit). The inner unit is represented by sets of beach ridges.

The equilibrium between coastal geometry and hydrodynamic regime determines the trapping potential of sand in a coastal segment. Sedimentary bypass is favored when equilibrium conditions are achieved. In this case, the reduction or interruption of coastal progradation would be an intrinsic condition of the coastal system. This mechanism was evoked by Blivi et al. (2002) to explain the interruption of progradation in a West Africa barrier (Benin). However, equilibrium conditions over long time intervals have not been achieved by the Ilha Comprida barrier system because the slow-down of progradation appears to be more related to coastal erosion than to simple coastline stability due to sediment bypassing.

Lessa et al. (2000) proposed the existence of a south–north littoral drift system in the coastal sector southward of the Ilha Comprida barrier. For these authors, the northward widening of the barriers would indicate an increasing potential of sand deposition from south to north. The northward transport of sediments would not be interrupted along the coastline due the presence of well-developed ebb tidal deltas at estuary mouths and headlands with shallow depth seabeds, both permitting sediment bypassing (Lessa et al., 2000). The dominant northward alongshore growth of the Ilha Comprida barrier, as evidenced by its beach ridge morphology (Geobrás, 1966; Martin and Suguio, 1978b; Guedes, 2003; Giannini et al., 2008) and its greater area, when compared with the southward barriers, allow to assume an extension of this south–north littoral drift system to the Ilha Comprida setting. In this case, morphodynamics changes of the barrier could be connected to changes in the regional littoral drift system. Holocene barrier progradation southward of Ilha Comprida (Paranaguá barrier) was very fast during the last thousand years (Lessa et al., 2000). Increasing deposition in the Paranaguá barrier could reduce the Ilha Comprida barrier progradation. But the progradation of the Ilha Comprida barrier varied considerably during the last thousand years (middle and outer units). On the other hand, the lack of detailed chronological data for these southward barriers does not allow a more precise comparison.

As discussed in Section 4.2, the middle unit comprises a period of wave erosion, with high foredunes and blowouts generated by S and SE winds, which are more active during the northward advance of cold fronts. Cold fronts are more intense during the winter and their passage through the southern and southeastern Brazilian coast increases the velocity of the S and SE winds as well as the height of S and SE waves (Rodrigues et al., 2004). Storm surges become more frequent, favoring coastal erosion but also the intensification of the northward alongshore currents and the sediment supply to some coastal segments. These conditions combined (S and SE winds with higher velocity, stable/erosion coastline and higher sediment supply) would favor the development of high foredunes and blowouts. The formation of foredunes and blowouts traps foreshore sediments in the backshore zone, diminishing coastal progradation. In this case, the decreasing progradation rate would be a consequence of the climate-controlled formation of foredunes and blowouts. Thus, it can be suggested that the coastal erosion, high foredunes and blowouts of the middle unit are indicative of a time period with more frequent and/or intense cold fronts advancing northward. Coastal morphological changes induced by climate fluctuations were also interpreted for the Keppel Bay barrier (Queensland, Australia) by Brooke et al. (2008b). The passage from the middle to the outer unit would be characterized by the continuation of enhanced southern winds and waves, but with minor intensity and/or higher sediment supply in the Ilha Comprida barrier segment. The trap potential of sand in the Ilha Comprida segment could be increased after the opening of the Valo Grande artificial channel in 1852 AD,

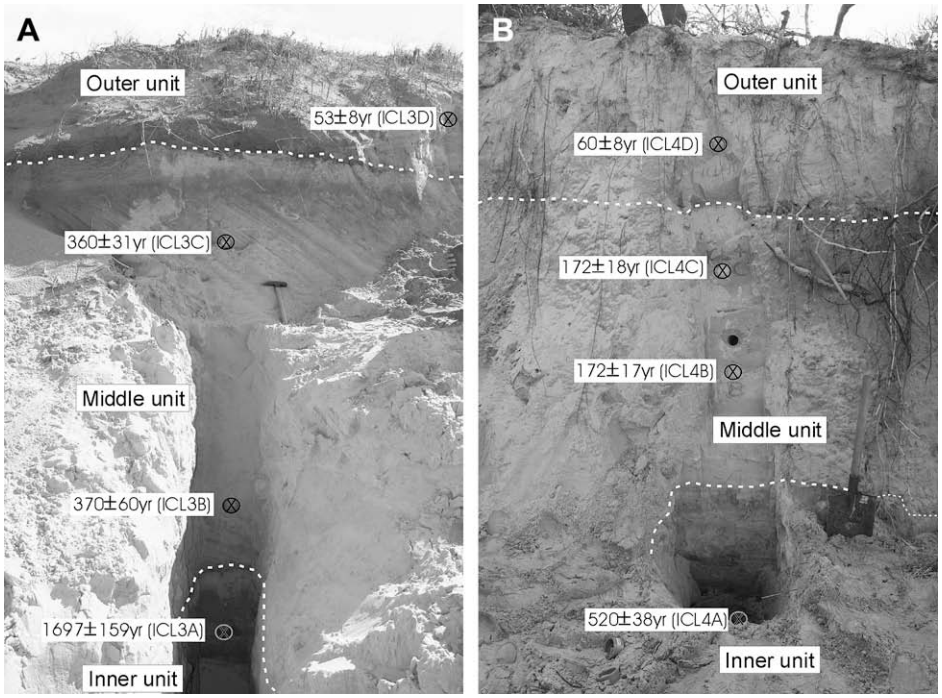

Fig. 12. Luminescence ages of the inner, middle and outer units vertically stacked at sites ICL3 (A) and ICL4 (B). No age differences are observed when samples from the same set of eolian sand facies are compared (samples ICL3B versus ICL3C and sample ICL4B versus ICL4C). Significant age differences are observed only between samples of different geomorphological units, which are separated by paleosol horizons or erosion surfaces.

which significantly elevated the ebb hydraulic jet at the Icapara inlet (Pisetta, 2006). In this way, the higher progradation rates of the outer unit would result from a human perturbation in the coastal system. The relative time synchronicity between the opening of the Valo Grande channel and the beginning of the outer unit favors this hypothesis.

5.3. Blowouts and foredunes of the Ilha Comprida barrier: connections with the Little Ice Age climatic event

Regardless of many factors that are able to affect the Ilha Comprida barrier progradation, the main morphological change (beach ridge dominated to foredune/blowouted ridge dominated) appears to be climate controlled. The blowouts of the middle unit developed from AD 1430 ± 47 to 1833 ± 18 (ages from 575 ± 47 to 172 ± 18 years), which is well correlated with the Little Ice Age (LIA) climatic event of AD 1450–1850 (Eddy, 1976). The LIA climate sensu Matthews and Briffa (2005) corresponds to a period when northern hemisphere summer temperatures fell below the mean of the AD 1961–1990. The global character of the LIA changes is relatively well accepted, with many events recognized in the south hemisphere (Thompson et al., 1986; Luckman and Villalba, 2001; Holmgren et al., 2003; Behling et al., 2004; Cohen et al., 2005; Unkel et al., 2007; Ariztegui et al., 2007). Although it was a global climate event, the LIA effects varied geographically. Despite the occurrence of many high frequency climate changes after the Middle Holocene, Kreutz et al. (1997) argued that the LIA provoked the major change in atmospheric circulation in the last 4000 years, which persisted into the 20th century. The LIA was a period with cold and warm anomalies and increased atmospheric circulation (Thompson et al., 1986; O'Brien et al., 1995; Shulmeister et al., 2004). According to Kreutz et al. (1997), both polar regions showed regional atmospheric circulation fluctuations with similar magnitude and timing, which occurred abruptly and affected low to middle latitude atmospheric circulation. Thompson et al. (1986) interpreted increased wind velocity across the high altiplano of southern Peru. Based on times taken by ships to sail from the Cape of Good Hope to St. Helena Island (South Atlantic), Farrington et al. (1998) deduced that both wind speed and steadiness of the Southeast Trades in the western African coast increased during the LIA. Lamy et al. (2001) recognized a northward shift of the southern westerlies in southern Chile during the LIA.

Table 3
Progradation rates calculated for profiles across foredune ridges

Segment	Distance (m)	Age interval (years)	Minimum rate (m/year)	Mean rate (m/year)	Maximum rate (m/year)	Depositional unit
Lagoon side to ICL1	3124	5308–4877[a] to 1004 ± 88	0.71	0.76	0.82	Inner
ICL1B-coastline	102	108 ± 10 to present	0.86	0.94	1.04	Outer
ICL5[b]-coastline	250	489 ± 48 to present	0.47	0.51	0.57	Middle and outer grouped
ICL8B-coasltine	379	187 ± 17 to present	1.86	2.03	2.23	Outer
ICL9C[b]-coastline	825	222 ± 23 to present	3.37	3.72	4.15	Middle and outer grouped
Lagoon side to coastline	3330	5308–4877[a] to present	0.63	0.65	0.68	Inner, middle and outer grouped

[a] Calibrated radiocarbon age of an in situ wood trunk from a muddy facies below plan parallel sand facies (foreshore) outcropping at the lagoon side of Ilha Comprida barrier (Guedes, 2003; Giannini et al., 2003a).
[b] Ages of blowouts give estimates of maximum rates.

Table 4
Progradation rates for coastal barriers from United States of America, Denmark, Spain, Australia, New Zealand and Argentina

Site	Progradation rates (m/year)	Age interval (years or years BP)	Dating method	Author
Chukchi Sea NW Alaska, USA	0.68	3700 to present	^{14}C	Mason and Jordan (1993)
St. Vincent Island, NW of Florida, USA	0.9	~4000 to 370	OSL	Lopez and Rink (2007)
Merrit Island, Florida, USA	1.35	~4000 to 150	OSL	Rink and Forrest (2005)
Northern Jutland, Denmark	2.0	~2700 to 1000	OSL	Nielsen et al. (2006)
Gulf of Almería West Mediterranean, Spain	1.0	~7400 to 1100	^{14}C[a]	Goy et al. (2003)
	0.6	~500 to present		
Guinchen Bay, South Australia	7.8	~5400 to 5300	OSL	Bristow and Pucillo (2006)
	0.54	~5300 to 4400		
	0.43	~4400 to 1800		
Guinchen Bay, South Australia	0.39	~5400 to 51	OSL	Murray-Wallace et al. (2002)
Beachmere, Queensland, Australia	0.32	~1700 to present	OSL	Brooke et al. (2008a)
	0.16	~1700 to 1140		
	0.41	~1140 to 190		
	1.06	~190 to present		
Keppel Bay, Queensland, Australia	1.2	~1500 to present	OSL	Brooke et al. (2008b)
	1.7	~1705 to 1335		
	4.3	~255 to 200		
	1.7	~100 to present		
Iluka Bay, Australia	1.3	~2900 to 2120	OSL and ^{14}C	Goodwin et al. (2006)
	0.9	~2120 to 1660		
Wood Bay, Autralia	0.7	~2400 to 1620		
	0.9	~1620 to 1420		
	0.45	~500 to 230		
	>1.0	~230 to 100		
	0.6	~500 to present		
Woy Woy, SW Australia	0.57	~7000 to 1500	^{14}C	Roy et al. (1994)
Wonboyn, SW Australia	0.38	~6800 to 1000		
Fens, SW Australia	0.35	~6000 to 3000		
Moruya, SW Australia	0.34	~5000 to 1000		
Tuncurry, SW Australia	0.26	~7500 to 1500		
Shoalheaven, SW Australia	0.24	~6500 to 2000		
North Canterbury, New Zealand	0.66	3810 to 2895	^{14}C	Shulmeister and Kirk (1997)
	0.25	2895 to 2090		
Coast from Rakaia River to Conway River, New Zealand	0.8	~130 to present	^{14}C	Worthington (1991)
San Sebastían Bay, Argentina	0.7	5270 to 975	^{14}C	Isla and Bujalesky (2000)
	1.0	4070 to 975		

[a] Calibrated radiocarbon age.

The timing of the LIA and increased southern winds in southeastern Brazil is consistent with the paleoclimate records obtained by Moy et al. (2008), who proposed the intensification of westerlies in SW Patagonia during the LIA. Northward incursions of cold air masses in subtropical Brazil became more frequent and intense during the Last Glacial Maximum due to higher latitudinal temperature gradients (Cruz et al., 2006). This assumption suggests that high latitude events of cooling correlate with more frequent and intense cold fronts migrating northward. As proposed by Cruz et al. (2006) on a 1000 years timescale, the enhancement of cold fronts in subtropical Brazil due to the high latitude cooling would also operate on a hundred years timescale. The enhancement of the South Atlantic atmospheric circulation occurred during the LIA would persist until present as it is indicated by the continued development of foredunes of the outer unit.

6. Conclusions

(1) Optically stimulated luminescence dating has been shown to be a suitable technique to study coastal depositional dynamics on a few thousand to hundred years timescale.
(2) Three geomorphological units were identified in the seaward portion of the Ilha Comprida barrier. The inner unit comprises low relief beach ridges, with ages greater than 1004 ± 88 years. The middle unit is characterized by higher foredunes disrupted by NNW blowouts. The blowout lobes dated to 575 ± 47 to 172 ± 18 years. The outer unit is characterized by a series of low foredunes and a small transgressive dunefield (migrating to NNW) at the northernmost portion of the barrier. The samples from this unit were younger than 108 ± 10 years. The successive character of the sedimentation of these three geomorphological units allows considering them as depositional units.
(3) The beach ridges, foredunes and blowouts are landforms resulting from relatively fast depositional processes characterized by short-time periods of sedimentation separated by long-time periods of non-deposition and soil formation. This is in agreement with the view of sedimentation as a discontinuous non-uniform process.
(4) The progradation rates in the Ilha Comprida barrier vary across the shore as well as alongshore. The ranges of progradation

Table 5
Descriptive statistics of progradation rates of coastal barriers from United States of America, Denmark, Spain, Australia, New Zealand and Argentina

Setting	Mean	Standard deviation	1° Quartile	Median	3° Quartile	Minimum	Maximum	*N*
All (10^2 years)	0.80	0.46	0.47	0.68	1.02	0.16	1.70	16
All (10^3 years)	0.71	0.48	0.34	0.57	1.00	0.24	2.00	17
Australia (10^2 years)	0.87	0.50	0.47	0.80	1.24	0.16	1.70	12
Australia (10^3 years)	0.45	0.28	0.30	0.36	0.46	0.24	1.20	10

Statistics of the data are presented in Table 4. 10^2 years and 10^3 years represent timescales of a 100 and 1000 years, respectively. The statistics of the progradation rates are in m/year.

rates obtained for the Ilha Comprida barrier are 0.71–0.82 m/year (inner unit) and 0.86–2.23 m/year (outer unit).

(5) The period of blowout development (AD 1430 ± 47 to 1833 ± 18) correlates very well with the LIA climatic event (AD 1450 to 1850). Blowout development is attributed to an increasing intensity and/or frequency of cold fronts advancing northward. Thus, the middle depositional unit marks a major shift in coastal dynamics of the Ilha Comprida barrier linked with the enhancement of the atmospheric circulation due to the LIA climatic event. This enhancement persisted to the present and is responsible for the formation of the eolian landforms in the outer unit.

(6) Barrier sedimentation can be sensitive to global climate events. The sensitivity of depositional systems to Late Holocene climate changes is favored by the relative sea level stillstand of this time.

(7) The Late Holocene coastal dynamics of the Ilha Comprida barrier studied through OSL dating of depositional landforms help in the evaluation of the impact of future climate changes on coastal settings.

Acknowledgments

Dr. Sérgio Willians de Oliveira Rodrigues is acknowledged for his help in the field survey, especially by his driver skills. The authors also wish to thank Dr. Nilberto Medina for the use of the HPGe detectors for gamma spectrometry. Dr. Francisco William da Cruz Jr. and Dr. Cristiano Mazur Chiessi are acknowledged for the information regarding the Holocene climate changes. André Oliveira Sawakuchi is very grateful to Dr. Gabriel Oliveira Sawakuchi, Dr. Eduardo Yukihara, Dr. Juan Mitani and M.Sc. David Klein for the assistance during his stay at the Radiation Dosimetry Laboratory (Oklahoma State University). We thank Dr. Thomas Rich Fairchild for English language suggestions on the manuscript.

We are also grateful to Dr. Duncan M. FitzGerald and two anonymous referees, who provided very constructive comments on the manuscript.

This work was funded by Fundação de Amparo à Pesquisa do Estado de São Paulo (FAPESP 01/01732-8 and 06/54649-4).

References

Adamiec, G., Aitken, M.J., 1998. Dose-rate conversion factors: update. Ancient TL 16, 37–50.

Aitken, M.J., 1998. Optical Dating. Academic Press, London.

Angulo, R.J., 1994. Indicadores morfológicos e sedimentológicos de paleoníveis marinhos quaternários na costa paranense. Boletim Paranaense de Geociências 42, 185–202.

Angulo, R.J., Lessa, G., 1997. The Brazilian sea level curves: a critical review with emphasis on the curves from Paranaguá and Cananéia regions. Marine Geology 140, 141–166.

Angulo, R.J., Giannini, P.C.F., Suguio, K., Pessenda, L.C.R., 1999. Relative sea-level changes in the last 5500 years in southern Brazil (Laguna–Imbituba region, Santa Catarina State) based on vermetid ^{14}C Ages. Marine Geology 159, 323–339.

Angulo, R.J., Pessenda, L.C.R., de Souza, M.C., 2002. O significado das datações ao ^{14}C na reconstrução de paleoníveis marinhos e na evolução das barreiras quaternárias do litoral paranaense. Revista Brasileira de Geociências 32, 95–106.

Angulo, R.J., Lessa, G.C., Souza, M.C., 2006. A critical review of mid- to late-Holocene sea-level fluctuations on the eastern Brazilian coastline. Quaternary Science Reviews 25, 486–506.

Ariztegui, D., Bosch, P., Davaud, E., 2007. Dominant ENSO frequencies during the Little Ice Age in Northern Patagonia: the varved record of proglacial Lago Frías, Argentina. Quaternary International 161, 46–55.

Barbouti, A., Rastin, B., 1983. A Study of the absolute intensity of muons at sea level and under various thicknesses of absorber. Journal of Physics G: Nuclear Physics 9, 1577–1595.

Behling, H., Pillar, V.D., Ci, L.O., Bauermann, S.G., 2004. Late Quaternary Araucaria forest, grassland (campos), fire and climate dynamics, studied by high-resolution pollen, charcoal and multivariate analysis of the Cambara do Sul core in southern Brazil. Palaeogeography, Palaeoclimatology, Palaeoecology 203, 277–297.

Blivi, A., Anthony, E.J., Oyédé, L.M., 2002. Sand barrier development in the bight of Benin, West Africa. Ocean & Coastal Management 45, 185–200.

Bøtter-Jensen, L., McKeever, S.W.S., Wintle, A.G., 2003. Optically Stimulated Luminescence Dosimetry. Elsevier, Amsterdam.

Bristow, C.S., Pucillo, K., 2006. Quantifying rates of coastal progradation from sediment volume using GPR and OSL: the Holocene fill of Guichen Bay, southeast South Australia. Sedimentology 53, 769–788.

Brooke, B.P., Lee, R., Cox, M., Olley, J., Pietsch, T., 2008a. Rates of shoreline progradation during the last 1700 years at Beachmere, southeastern Queensland, Australia, based on OSL dating of beach ridges. Journal of Coastal Research 24 (3), 640–648.

Brooke, B.P., Ryan, D., Pietsch, T., Olley, J., Douglas, G., Packett, R., Radke, L., Flood, P., 2008b. Influence of climate fluctuations and changes in catchment land use on Late Holocene and modern beach-ridge sedimentation on a tropical macrotidal coast: Keppel Bay, Queensland, Australia. Marine Geology 251, 195–208.

CTH-USP (Centro Tecnológico de Hidráulica da Escola Politécnica da Universidade de São Paulo), 1973. Observações das características das ondas do mar em Cananéia. Technical Report. CTH-USP, DAEE, São Paulo, Brazil.

Cohen, M.C.L., Behling, H., Lara, R.J., 2005. Amazonian mangrove dynamics during the last millennium: the relative sea-level and the Little Ice Age. Review of Palaeobotany and Palynology 136, 93–108.

Corrêa, I.C.S., 1996. Les variations du niveau de la mer durant les derniers 17.500 ans BP: l'exemple de la plateforme continentale du Rio Grande do Sul-Brésil. Marine Geology 130, 163–178.

Cowell, P.J., Stive, M.J.F., Niedoroda, A.W., Vriendde, H.J., Swift, D.J.P., Kaminsky, G.M., Capobianco, M., 2003a. The coastal tract (Part 1): a conceptual approach to aggregated modeling of low-order coastal change. Journal of Coastal Research 19 (4), 812–827.

Cowell, P.J., Stive, M.J.F., Niedoroda, A.W., Swift, D.J.P., de Vriend, H.J., Buijsman, M.C., Nicholls, R.J., Roy, P.S., Kaminsky, G.M., Cleveringa, J., Reed, C.W., de Boer, P.L., 2003b. The coastal tract (part 2): applications of aggregated modeling of low-order coastal changes. Journal of Coastal Research 19 (4), 828–848.

Cruz Jr., F.W., Burns, S.J., Karmann, I., Sharp, W.D., Vuille, M., Ferrari, J.A., 2006. A stalagmite record of changes in atmospheric circulation and soil processes in the Brazilian subtropics during the Late Pleistocene. Quaternary Science Reviews 25, 2749–2761.

Delibrias, C., Laborel, J., 1969. Recent variations of the sea level along the Brazilian coast. Quaternaria 14, 45–49.

De Maman, Y.J., 2006. Análise sedimentológica aplicada na mineração de areia no Vale do Ribeira – região de Registro, SP. Monography. Instituto de Geociências, Universidade de São Paulo, São Paulo, Brazil.

(Departamento de Águas e Energia Elétrica do Estado de São Paulo), D.A.E.E., 1998. Bacia Hidrográfica do Ribeira de Iguape – Plano de Ação para o Controle das Inundações e Diretrizes para o Desenvolvimento do Vale. Technical Report. DAEE, São Paulo, Brazil.

Duller, G.A.T., 1995. Luminescence measurements using single aliquots: methods and applications. Radiation Measurements 24, 217–226.

Eddy, J.A., 1976. The Maunder Minimum. Science 192, 1189–1202.

Farrington, A.J., Lubker, S., Radok, U., Woodruff, S., 1998. South Atlantic winds and weather during and following the Little Ice Age – a pilot study of English East India Company (EEIC) ship logs. Meteorology and Atmospheric Physics 67, 253–257.

Flexor, J.M., Martin, L., Suguio, K. 1979. Utilization du rapport isotopique $^{13}C/^{12}C$ comme indicateur d'oscillations lagunaires. Proceedings of the International Symposium on Coastal Evolution in the Quaternary, São Paulo, Brazil, pp. 356–375.

Geobrás, S.A., 1966. Complexo Valo Grande, Mar Pequeno e Rio Ribeira de Iguape. Technical Report, Relatório GEOBRÁS S.A., 2 volumes. Engenharia e Fundações para o Serviço do Vale do Ribeira do Departamento de Águas e Energia Elétrica/SP, Brazil.

Giannini, P.C.F., Guedes, C.C.F., Angulo, R.J., Assine, M.L., Souza, M.C., Mori, E.K., 2003a. Geometria de cordões litorâneos e espaço de acomodação sedimentar na ilha Comprida, litoral sul paulista: modelo baseado em aerofotointerpretação. In: IX Congresso da Associação Brasileira de Estudos do Quaternário, Brasil (cd).

Giannini, P.C.F., Guedes, C.C.F., Assine, M.L., Angulo, R.J., Souza, M.C., Pessenda, L.C.R., 2003b. Variação longitudinal e transversal de propriedades sedimentológicas nos cordões litorâneos da Ilha Comprida, litoral sul paulista. In: IX Congresso da Associação Brasileira de Estudos do Quaternário, Recife, Brasil (cd).

Giannini, P.C.F., Guedes, C.C.F., Nascimento Jr., D.R., Tanaka, A.P.B., Angulo, R.J., Assine, M.L., Souza, M.C., 2008. Sedimentology and morphologic evolution of the Ilha Comprida Barrier System, southern São Paulo coast. In: Dillenburg, S.R., Hesp, P. (Eds.), Geology of the Brazilian Coastal Barriers. Lecture Notes in Earth Sciences. Springer-Verlag, Heidelberg.

Goodwin, I.D., Stables, M.A., Olley, J.M., 2006. Wave climate, sand budget and shoreline alignment evolution of the Iluka–Woody Bay sand barrier, northern New South Wales, Australia, since 3000 yr BP. Marine Geology 226, 127–144.

Goy, J.L., Zazob, C., Dabrio, C.J., 2003. A beach-ridge progradation complex reflecting periodical sea-level and climate variability during the Holocene (Gulf of Almería, Western Mediterranean). Geomorphology 50, 251–268.

Guedes, C.C.F., 2003. Os cordões litorâneos e as dunas eólicas da Ilha Comprida, Estado de São Paulo. Monography. Instituto de Geociências, Universidade de São Paulo, São Paulo, Brazil.

Harari, J., França, C.A.S., Camargo, R., 2004. Variabilidade de longo termo de componentes de marés e do nível médio do mar na costa brasileira. Afro-America Gloss News 8 (1).

Hesp, P., 1999. The beach backshore and beyond. In: Short, A.D. (Ed.), Handbook of Beach and Shoreface Morphodynamics. John Wiley & Sons, Chichester, pp. 145–170.
Hesp, P., 2002. Foredunes and blowouts: initiation, geomorphology and dynamics. Geomorphology 48, 245–268.
Hesp, P., Dillenburg, S.R., Barboza, E.G., Tomazelli, L.J., Ayup-Zouain, R.N., Esteves, L.S., Gruber, N.L.S., Toldo- Jr., E.E., Tabajara, L.L.C.A., Clerot, L.C.P., 2005. Beach ridges, foredunes or transgressive dunefields? Definitions and an examination of the Torres to Tramandaí barrier system, Southern Brazil. Anais da Academia Brasileira de Ciências 77 (3), 493–508.
Holmgren, K., Lee-Thorp, J.A., Cooper, G.R.J., Lundblad, K., Partridge, T.C., Scott, L., Sithaldeen, R., Talma, A.S., Tyson, P.D., 2003. Persistent millennial-scale climatic variability over the past 25,000 years in Southern Africa. Quaternary Science Reviews 22, 2311–2326.
IBGE (Instituto Brasileiro de Geografia e Estatística), 1992. Atlas Nacional do Brasil. IBGE, Rio de Janeiro.
IPCC-DCC, 2000. ipcc-dcc.cptec.inpe.br/ipccddcbr/hlml/asres/secario_home.html.
Isla, F.I., Bujalesky, G.G., 2000. Cannibalisation of Holocene gravel beach-ridge plains, northern Tierra del Fuego, Argentina. Marine Geology 170, 105–122.
Korvin, G., 1992. Fractal Models in the Earth Sciences. Elsevier, Amsterdam.
Kowsmann, R.O., Costa, M.P.A., 1979. Sedimentação quaternária da margem continental brasileira e das áreas oceânicas adjacentes. Technical Report, v.8, REMAC Project (Reconhecimento Global da Margem Continental Brasileira). PETROBRÁS-DNPM-CPRM-DHN-CNPq, Brazil.
Kreutz, K.J., Mayewski, P.A., Meeker, L.D., Twickler, M.S., Whitlow, S.I., Pittalwala, I.I., 1997. Bipolar changes in atmospheric circulation during the Little Ice Age. Science 277, 1294–1296.
Lamy, F., Hebbeln, D., Röhl, U., Wefer, G., 2001. Holocene rainfall variability in southern Chile: a marine record of latitudinal shifts of the Southern Westerlies. Earth and Planetary Science Letters 185, 369–382.
Lessa, G.C., Angulo, R.J., Giannini, P.C., Araújo, A.D., 2000. Stratigraphy and Holocene evolution of a regressive barrier in south Brazil. Marine Geology 187, 87–108.
Lian, O.B., Roberts, R.G., 2006. Dating the Quaternary: progress in luminescence dating of sediments. Quaternary Science Reviews 25, 2449–2468.
Lopez, G.I., Rink, W.J., 2007. Characteristics of the burial environment related to quartz SAR-OSL dating at St. Vincent Island, NW Florida, USA. Quaternary Geochronology 2, 65–70.
Luckman, B.H., Villalba, R., 2001. Assessing the synchroneity of glacier fluctuations in the western cordillera of the Americas during the last millennium. In: Markgraf, V. (Ed.), Interhemispheric Climate Linkages. Academic Press, New York, pp. 119–137.
Madsen, A.T., Murray, A.S., Andersen, T.J., Pejrup, M., Breuning-Madsen, H., 2005. Optically stimulated luminescence dating of young estuarine sediments: a comparison with ^{210}Pb and ^{137}Cs dating. Marine Geology 214, 251–268.
Martin, L., Suguio, K., 1978a. Excursion rout along the coastline between the town of Cananéia (State of São Paulo) and Guaratiba outlet (State of Rio de Janeiro). In: International Symposium on Coastal Evolution in the Quaternary, Special Publication, São Paulo, Brazil, pp. 1–98.
Martin, L, Suguio, K., 1978b. Ilha Comprida: um exemplo de ilha barreira ligada às flutuações do nível marinho durante o Quaternário. XXX Congresso Brasileiro de Geologia, Recife, Brazil, 2, pp. 905–912.
Martin, L., Suguio, K., 1989. Excursion route along the Brazilian coast between Santos (SP) and Campos (RJ) (North of State of Rio de Janeiro). International Symposium on Global Changes in South America During the Quaternary, v.2, Special Publication, São Paulo, Brazil, pp. 1-136.
Martin. L., Suguio, K., Flexor, J.M., 1979. Le Quaternaire marin du littoral bresilien entre Cananéia (SP) et Barra de Guaratiba (RJ). In: Proceedings of the International Symposium on Coastal Evolution in the Quaternary, São Paulo, Brazil, pp. 296–331.
Martin, L., Suguio, K., Flexor, J.M., Bittencourt, A.C.S.P., Vilas-Boas, G.S., 1979/1980. Le quaternaire marin brésilien (littoral pauliste, sud fluminense et bahianais). Cahiers O.R.S.T.O.M., Série Géologie 11, 95–124.
Martin, L., Suguio, K., Flexor, J.N., 1988. Hauts niveaux marins pleistocenes du litoral bresilien. Palaeogeography Palaeoclimatology. Palaeoecology 68 (3), 231–239.
Martin, L., Suguio, K., Flexor, J.M., Dominguez, J.M.L., Bittencourt, A.C.S.P., 1996. Quaternary sea-level history and variation in dynamics along the central Brazil Coast: consequences on coastal plain construction. Anais da Academia Brasileira de Ciências 68, 303–354.
Martin, L., Suguio, K., Dominguez, J.M.L., Flexor, J.M., 1997. Geologia do Quaternário costeiro do litoral norte do Rio de Janeiro e do Espírito Santo. Technical Report. CPRM Serviço Geológico do Brasil, Brazil, 112 pp.
Mason, O.K., Jordan, J.W., 1993. Heightened North Pacific Storminess during synchronous Late Holocene of Northwest Alaska beach ridges. Quaternary Research 40, 55–69.
Matthews, J.A., Briffa, K.R., 2005. The 'Little Ice Age': re-evaluation of an evolving concept. Geografiska Annaler 87A, 17–36.
Milne, G.A., Mitrovica, J.X., Davis, J.L., 1999. Near-field hydro-isostasy: the implementation of a revised sea-level equation. Geophysical Journal International 139, 464–482.
Moy, C.M., Dunbar, R.B., Moreno, P.I., Francois, J-P., Villa-Martinez, R., Mucciarone, D.M., Guilderson, T.P., Garreaud, R.D., 2008. Isotopic evidence for hydrologic change related to the westerlies in SW Patagonia, Chile, during the last millenium. Quaternary Science Reviews 27, 1335–1349.
Murray, A.S., Wintle, A.G., 2000. Luminescence dating of quartz using an improved single-aliquot regenerative-dose protocol. Radiation Measurement 32, 57–73.
Murray-Wallace, C.V., Banerjee, R.P., Bourman, J.M., Olley, J.M., Brooke, B.P., 2002. Optically stimulated luminescence dating of Holocene relict foredunes, Guichen Bay, South Australia. Quaternary Science Review 21, 1077–1086.
Nascimento, D.R. Jr., 2006. Morfologia e sedimentologia ao longo do sistema praia – duna frontal de Ilha Comprida, SP. Master dissertation, Instituto de Geociências, Universidade de São Paulo, São Paulo, Brazil.
Nielsen, A., Murray, A.S., Pejrup, M., Elberling, B., 2006. Optically stimulated luminescence dating of a Holocene beach ridge plain in Northern Jutland, Denmark. Quaternary Geochronology 1, 305–312.
Nimer, E., 1989. Climatologia do Brasil. IBGE, Rio de Janeiro.
Nogués-Paegle, J., Mo, K.C., 1997. Alternating wet and dry conditions over South America during summer. Monthly Weather Review 125, 279–291.
O'Brien, S.R., Mayewski, P.A., Meeker, L.D., Meese, D.A., Twicker, M.S., Whitlow, S.I., 1995. Complexity of Holocene climate as reconstructed from a Greenland ice core. Science 270, 1962–1964.
Otvos, E.G., 2000. Beach ridges – definitions and significance. Geomorphology 32, 83–108.
Pietsch, T.J., Olley, J.M., Nanson, G.C., 2008. Fluvial transport as a natural luminescence sensitiser of quartz. Quaternary Geochronology 3, 365–376.
Pisetta, M., 2006. Transporte de sedimentos por suspensão no sistema estuarino-lagunar de Cananéia-Iguape (SP). Master dissertation, Instituto Oceanográfico, Universidade de São Paulo, São Paulo, Brazil.
Prescott, J.R., Stephan, L.G., 1982. The contribution of cosmic radiation to the environmental dose for thermoluminescence dating. In: Proceedings of the Second Specialist Seminar on Thermoluminescence Dating 6, Council of Europe, Strasbourg, pp. 17–25.
Reinson, G.E., 1979. Barrier island systems. In: Walker, R.G. (Ed.), Facies Models. Geoscience Canada, Ottawa, pp. 57–74.
Rink, W.J., Forrest, B., 2005. Dating evidence for the accretion history of beach ridges on Cape Canaveral and Merritt Island, Florida, USA. Journal of Coastal Research 21, 1000–1008.
Rodrigues, M.L.G., Franco, D., Sugahara, S., 2004. Climatologia de frentes frias no litoral de Santa Catarina. Revista Brasileira de Geofísica 22 (2), 135–151.
Roy, P.S., Cowell, M.A., Ferland, M.A., Thom, B.G., 1994. Wave-dominated coasts. In: Carter, R.W.G., Woodroffe, C.D. (Eds.), Coastal Evolution – Late Quaternary Shoreline Morphodynamics. Cambridge University Press, Cambridge, pp. 121–186.
Sadler, P.M., 1981. Sediment accumulation rates and the completeness of stratigraphic sections. Journal of Geology 89, 569–584.
Satyamurti, P., Nobre, C., Dias, P.L.S., 1998. South America. In: Karoly, D.J., Vicent, D.J. (Eds.), Meteorology of the Southern Hemisphere. American Meteorological Society, Boston, pp. 119–139.
Seluchi, M.E., Marengo, J.A., 2000. Tropical-midlatitude exchange of air masses during summer and winter in South America: climatic aspects and examples of intense events. International Journal of Climatology 20, 1167–1190.
Shulmeister, J., Kirk, R.M., 1997. Holocene fluvial–coastal interactions on a mixed sand and gravel beach system, North Canterbury, New Zealand. Catena 30, 337–355.
Shulmeister, J., Goodwin, I., Renwick, J., Harle, K., Armand, L., McGlone, M.S., Cook, E., Dodson, J., Hesse, P.P., Mayewskim, P., Curran, M., 2004. The southern hemisphere westerlies in the Australasian sector over the last glacial cycle: a synthesis. Quaternary International 118-119, 23–53.
Suguio, K., Martin, L., 1978a. Mapas geológicos da planície costeira do Estado de São Paulo e sul do Rio de Janeiro (1:100.000). Technical Report. DAEE/Secret. de Obras e Meio Ambiente, Gov. do Estado de São Paulo, São Paulo, Brazil.
Suguio, K., Martin, L., 1978b. Formações quaternárias marinhas do litoral paulista e sul fluminense. In: International Symposium on Coastal Evolution in the Quaternary – The Brazilian National Working Group for the IGCP, Project 61, Special Publication, São Paulo, Brazil, pp. 1–55.
Suguio, K., Martin, L., Bittencourt, A.C.S.P., Dominguez, J.M.L., Flexor, J.M., Azevedo, A.E.G., 1985. Flutuações do nível relativo do mar durante o Quaternário Superior ao longo do litoral brasileiro e suas implicações na sedimentação costeira. Revista Brasileira de Geociências 15 (4), 273–328.
Suguio, K., Tatumi, S.H., Kowata, E.A., 1999. As cristas de dunas inativas e os seus possíveis significados na evolução holocênica da Ilha Comprida, sul do litoral paulista. In: VII Congresso da Associação Brasileira de Estudos do Quaternário, Porto Seguro, Brasil (cd).
Suguio, K., Tatumi, S.H., Kowata, E.A., Munita, C.S., Paiva, R.P., 2003. Upper Pleistocene deposits of the Comprida Island (São Paulo State) dated by thermoluminescence method. Anais da Academia Brasileira de Ciências 75 (1), 91–96.
Tessler, M.G., 1982. Sedimentacão atual na região lagunar de Cananeia-Iguape, Estado de São Paulo. Master dissertation, Instituto de Geociências, Universidade de São Paulo, São Paulo, Brazil.
Tessler, M.G., 1988. Dinâmica Sedimentar Quaternária no Litoral Sul Paulista. PhD thesis, Instituto de Geociências, Universidade de São Paulo, São Paulo, Brazil.
Thompson, L.G., Mosley-Thompson, E., Dansgaard, W., Grootes, P.M., 1986. The Little Ice Age as recorded in the stratigraphy of the tropical Quelccaya ice cap. Science 234, 361–364.
Unkel, I., Kadereit, A., Machtle, B.M., Eitel, B., Kromer, B., Wagner, G., Wacker, L., 2007. Dating methods and geomorphic evidence of palaeonvironmental changes at the eastern margin of the South Peruvian coastal desert (14°30′S) before and during the Little Ice Age. Quaternary International 175, 3–28.
Van Andel, T.H., Laborel, J., 1964. Recent high relative sea level stand near Recife, Brazil. Science 145, 580–581.
Wintle, A.G., Murray, A.S., 2006. A review of quartz optically stimulated luminescence characteristics and their relevance in single-aliquot regeneration dating protocols. Radiation Measurements 41, 369–391.
Worthington, A., 1991. Assessment of Coastal Erosion Potential Rakaia River to Conway River. Technical Report. Canterbury Regional Council Publ. R90/12, New Zealand.
Wright, L.D., Short, A.D., 1984. Morphodynamics variability of surf zones and beaches: a synthesis. Marine Geology 56, 93–118.